



Universidade de Lisboa
Instituto Superior Técnico

Eco-friendly cyclam based coatings for biofouling prevention

Inês Maria Maia Nunes

Thesis to obtain the Master of Science Degree in

Chemical Engineering

Supervisor: Dr. Luís Gonçalo Andrade Rodrigues Alves

Co-Supervisor: Dr. Elisabete Ribeiro Silva

Jury

Chairperson: Prof. Maria Matilde Soares Duarte Marques

Supervisor: Dr. Luís Gonçalo Andrade Rodrigues Alves

Member of the committee: Prof. Filipe José Menezes Mergulhão

December/2020

Abstract

Cyclam derivatives were synthesised, characterized, and incorporated into polyurethane-based coating formulations to create an alternative system for water bio-decontamination. The results showed that despite the proved antimicrobial potential of the cyclam-based antimicrobials, and those to be incorporated in silicone-based coatings to originate antimicrobial coatings, their behaviour changed after their incorporation in polyurethane (PU)-based formulations. PU coatings containing cyclam derivatives did not evidence significant antimicrobial effects against Methicillin-resistant *Staphylococcus aureus* and *Escherichia coli*. The lack of activity was associated with the high compatibility of the cyclam structural functionality that promoted their strong chemical binding with the polymeric coating matrix. Reactivity studies of the cyclam-derived compounds with 4,4'-methylene diphenyl diisocyanate (MDI), a representative isocyanate-based component of a PU-based formulation, revealed the formation of urethane- and urea-type bonds depending on the functionality of the pending arm present in the cyclam ring. This chemical compatibility of cyclam derivatives with polyurethane matrices also promoted their effective immobilization, avoiding any leaching of cyclam derivatives from submerged coated substrates into waters after a 45 days immersion period.

Keywords: Water bio-decontamination, bacteria, antimicrobial cyclams, immobilization, polyurethane coatings

This page was intentionally left blank.

Resumo

Derivados de ciclama foram sintetizados, caracterizados e incorporados em formulações de revestimento à base de poliuretano para criar um sistema alternativo para a bio-descontaminação da água. Os resultados mostraram que, apesar do comprovado potencial antimicrobiano dos antimicrobianos à base de ciclama, e daqueles a serem incorporados em revestimentos à base de silicone para originar revestimentos antimicrobianos, o seu comportamento mudou após a sua incorporação em formulações à base de poliuretano (PU). Os revestimentos de PU contendo derivados de ciclama não evidenciaram efeitos antimicrobianos significativos contra *Staphylococcus aureus* resistente à meticilina e *Escherichia coli*. A falta de atividade foi associada à alta compatibilidade da funcionalidade estrutural da ciclama que promoveu a sua forte ligação química com a matriz polimérica de revestimento. Estudos de reatividade dos compostos derivados de ciclama com 4,4'-metileno difenil diisocianato (MDI), um componente à base de isocianato representativo de uma formulação à base de PU, revelou a formação de ligações do tipo uretano e ureia, dependendo da funcionalidade do braço pendente presente no anel de ciclama. Esta compatibilidade química dos derivados de ciclama com matrizes de poliuretano também promoveu a sua efetiva imobilização, evitando qualquer lixiviação dos derivados de ciclama de substratos revestidos submersos em águas após um período de imersão de 45 dias.

Palavras-chave: Bio-descontaminação da água, bactérias, ciclamas antimicrobianos, imobilização, revestimentos de poliuretano

This page was intentionally left blank.

Acknowledgments

I would like to thank the following people for their valuable contribution, directly or indirectly related to this work. For being by my side during this journey, throughout the good and the less good moments.

First, I would like to express my sincere gratitude to both my supervisors Dr. Luís Alves and Dr. Elisabete Silva, for their scientific guidance, all the encouragement, commitment, concern and support throughout this research project, especially during the pandemic which we are living through. To my colleagues at the IST laboratory Patrícia, Vanessa, César, Cláudia, Tiago, Carina, Marta and Rita. Thank you for the moments and the support provided.

I would also like to thank Master Olga Ferreira for her support, availability and help at FCUL.

I am deeply indebted to my family, especially to my parents Isabel and Mário, my sister Leonor and my grandparents Adelina, Honorato, Irene and Bernardino for their permanent and unconditional support, encouragement, patience and for giving me the bases to overcome life's challenges.

I would like to thank my friends from Porto who have supported me since the beginning, especially when I had to come to Lisbon: Isabel Campos, Margarida Silva, Carolina Araújo, Inês Proença, Clara Costa, Margarida Guimarães, Bernardo Tavares, Francisco Perez, David Campos, Henrique Siza, Bernardo Gomes, Hugo Silva, Ricardo Ribeiro, Sara Santos and Carlos Neves.

I also want to thank my previous and current friends at IST, who I had the luck to encounter: Patrícia Pereira, Marisa Pereira, Jorge Rocha, Rita Costa, Diana Dimande, António Mesquita, Sara Coneição, Rita Fialho, Leonardo Pereira, Inês Cabral, João Rodrigues, Hugo Guerreiro, João Coelho and Catarina Louro. Thank you for always supporting me and encouraging me to do my best, without them I would not have been able to complete this stage of my life.

A very special thanks also to all people here in Lisbon who supported me when I came here. To Susana Malho for all the support given, especially in the first year, and to Paula Cardoso, Sofia Neves, Gonçalo Neves and João Neves for all their friendship and affection.

This page was intentionally left blank.

Acronyms

ACN – Acetonitrile

ATCC – American Type Culture Collection

ATR-IR – Attenuated Total Reflection-Infrared

Boc – *tert*-butoxycarbonyl

Boc₂O – *Di-tert*-butyl decarbonate

BRICS - Brazil, Russia, India, China, and South Africa

CA – Curing Agent

COSY – Correlation Spectroscopy

E. coli – *Escherichia coli*

FTIR – Fourier Transform Infrared Spectroscopy

HPLC-MS – High Performance Liquid Chromatography coupled to Mass Spectrometry

HSQC – Heteronuclear Single Quantum Correlation

IR – Infrared

ISO – International Organization for Standardization

mbar - Millibar

MDI – 4,4'-methylenediphenyldiisocyanate

MRSA – Methicillin-resistant *Staphylococcus aureus*

NCO – Isocyanate functional group

NMR – Nuclear Magnetic Resonance

OECD – Organisation for Economic Co-operation and Development

ORTEP – Oak Ridge Thermal Ellipsoid Plot

PDMS – Polydimethylsiloxane

ppm – Parts-per-million

PU – Polyurethane

PVC – Polyvinyl chloride

REF – Control coated reference plane

ROW – Rest of World

rpm – Revolutions per minute

TACN - 1,4,7-Triazacyclononane

THF – Tetrahydrofuran

VOCs – Volatile Organic Compounds

UNICEF – United Nations International Children's Emergency Fund

UV – Ultraviolet light

WHO – World Health Organization

wt. – Weight

WWAP – World Water Assessment

This page was intentionally left blank.

Index

Abstract	i
Resumo	iii
Acknowledgments	v
Acronyms	vii
1. Introduction	1
1.1. Water	1
1.1.1. Importance and pollution	1
1.1.2. Treatment	2
1.2. Water Biocontamination	4
1.2.1. Biofouling	4
1.2.2. Control and prevention of biofouling	6
1.3. Protective Coatings	7
1.3.1. General characteristics and classification of paints	7
2. Materials and methods	9
2.1. General Considerations	9
2.2. Characterization Techniques	9
2.3. Synthesis of compounds	10
2.4. Incorporation of cyclam compounds in polymeric coatings	15
2.5. Evaluation of antimicrobial activity of coatings containing cyclam derived compounds	15
2.6. Leaching tests	16
3. Results and Discussion	17
3.1. Synthesis of cyclam derivatives	17
3.1.1. Synthesis of <i>mono</i> -substituted cyclam derivatives	17
3.1.2. Synthesis of <i>trans</i> -di-substituted cyclam derivatives	18
3.1.3. Synthesis of <i>trans</i> -di-di-substituted cyclam derivatives	19
3.2. Incorporation of cyclam compounds in polymeric coatings	24
3.3. Evaluation of antimicrobial activity of coatings containing cyclam derived compounds	24
3.4. Reaction of <i>trans</i> -disubstituted cyclam derivatives with MDI	25
3.5. Leaching tests	27
4. Conclusions	29
References	31
Annexes	35

Figure Index

Figure 1. Representative scheme of the marine biofouling process. ^[20]	4
Figure 2. Biofouling on a ship's hull. Courtesy of Hempel's Marine Paints A/S. ^[24]	5
Figure 3. Biofouling on a cooling water pipe in the ship's system. ^[25]	5
Figure 4. PVC plaques coated with formulations containing a control coated reference plaque without any compound (REF) and the compounds 7 and 9	15
Figure 5. Leaching test of panels coated with the optimised formulations containing the compounds 7 , 9 and 11 and control coated reference panel submerged in distilled water.	16
Figure 6. ¹ H NMR spectrum of 7 in CDCl ₃ at 296K.	19
Figure 7. ORTEP diagram of (MeO(O)CCH ₂ CH ₂) ₂ (⁴ -CF ₃ PhCH ₂) ₂ Cyclam, 8 , showing thermal ellipsoids at 40% probability level. Selected hydrogen atoms are omitted for clarity.....	20
Figure 8. ORTEP diagram of (EtO(O)CCH ₂) ₂ (⁴ -CF ₃ PhCH ₂) ₂ Cyclam, 10 , showing thermal ellipsoids at 40% probability level. Selected hydrogen atoms are omitted for clarity.	20
Figure 9. ¹ H and ¹³ C{ ¹ H} NMR spectra of 9 in CDCl ₃ at 296K.	21
Figure 10. ¹ H and ¹³ C{ ¹ H} NMR spectra of 11 in CDCl ₃ at 296K.	22
Figure 11. ORTEP diagram of (HOCH ₂ CH ₂) ₂ (⁴ -CF ₃ PhCH ₂) ₂ Cyclam, 11 , showing thermal ellipsoids at 40% probability level. Selected hydrogen atoms are omitted for clarity. Dashed lines represent hydrogen bonds.....	22
Figure 12. ORTEP diagram of (NCCH ₂ CH ₂) ₂ (⁴ -CF ₃ PhCH ₂) ₂ Cyclam, 12 , showing thermal ellipsoids at 40% probability level. Selected hydrogen atoms are omitted for clarity.	23
Figure 13. Antimicrobial assessment of coatings containing a reference (Ref PU) Petri dish and the optimized formulations of compounds 7 , 9 and 11 against MRSA (left side of petri dishes) and E. coli strains (right side of petri dishes).	25
Figure 14. IR spectra of compound 7 (orange) and the obtained compound after functionalization of compound 7 with diisocyanate (blue).....	26
Figure 15. IR spectra of compound 9 (orange) and the obtained compound after functionalization of compound 9 with diisocyanate (blue).....	26
Figure 16. Proposed representative products obtained from the reaction of 7 and 9 with 4,4'-MDI.	27

Scheme Index

Scheme 1. Reaction scheme of the synthesis of <i>mono</i> -substituted cyclam derivative. (Compounds in grey were not successfully achieved)	17
Scheme 2. Reaction scheme of the synthesis of <i>trans</i> -di-substituted cyclam derivative.	18
Scheme 3. Reaction scheme of the synthesis of <i>trans</i> -di-di-substituted cyclam derivative.	20
Scheme 4. Reaction scheme of the synthesis of <i>trans</i> -di-di-substituted cyclam derivative 12 . ..	23

Table Index

Table 1. Advantages and drawbacks of different water treatment process. ^{[12],[15],[16]}	3
Table 2. Antibacterial coatings approaches. ^[28]	6
Table 3. Paints divided based on their physical form, according to the solvent and depending on their constituents. ^[37]	8
Table 4. Paints matrices in accordance with their solvent or ligand nature. ^[33]	8
Table 5. Optimized coating formulations containing cyclam-derived compounds 7 , 9 and 11 ...	24
Table A1. Crystal data and structure refinement for 8	35
Table A2. Crystal data and structure refinement for 10	36
Table A3. Crystal data and structure refinement for 11	37
Table A4. Crystal data and structure refinement for 12	38

This page was intentionally left blank.

1. Introduction

1.1. Water

1.1.1. Importance and pollution

Water is one of the most important substances and the main constituent of Earth being essential for some physiological processes in living organisms like body temperature regulation, nerve impulses transmission, as a component in the digestion of food or as a solvent in vital chemical reactions. Human beings, as living organisms are also very dependent on water. To survive, human population needs it not only to drink, but also for other uses such as cooking, washing and cleaning.^[1] About 70% of freshwater consumption on the planet is used in animal farming and agriculture, while 19% is used for industrial purposes and 11% is applied in municipal purposes.^{[2],[3]} This consumption tend to increase and is allied to another challenge, the water pollution. Water pollution occurs when hazardous substances contaminate a water source (stream, river, lake, ocean or aquifer) leading to its quality degradation. According to World Water Assessment Programme (WWAP), about 80% of the world's wastewater are released into the environment without adequate treatment, polluting rivers, lakes and oceans and thus, making it toxic to humans and to the ecosystems.^{[4],[5],[6]}

The main reason behind water pollution crisis, is its global threat to the public health, demanding for sustainable and environmentally friendly solutions. According to the World Health Organization (WHO), in 2016, gastrointestinal problems related to the use of contaminated water and sanitation problems were equivalent to about 3.6% of the global weight of daily diseases being responsible for the death of nearly 1.2 million people, including almost 300 000 of children aged under 5 years who died due to diarrhoea.^{[5],[7],[8]}

In the report prepared by UNICEF and WHO, which analyses the situation until 2016, it is indicated that only 2,900 million people (39% of the world population) have access to safe sanitary services and their sewage treatment.^[9] Thus, it is essential to develop simple, practical, and economical techniques for water decontamination.

The origin and quality of the water source are important aspects when deciding which treatment process should be performed. Whether the source comes from surface or underground will also depend on its treatment. Pollutants present in the soil, can originate from the transformation of natural products (rainwater, dust at the atmosphere, surrounding vegetation and underground rocks and volcanoes) or man-made due to domestic, agricultural or industrial activities.^[10]

The presence of pollutants in water can cause several problems like the lack of clean and safe water for consumption, hygiene, and sanitation, triggering outbreaks of serious diseases that may be lethal. Infectious diseases caused by the presence of microbial contaminants in drinking water like pathogenic bacteria, viruses and parasites (for example, protozoa and helminths) are one of the most common and widespread health risk to human health associated with drinking-water.^[11]

Microbial water pollution have several diseases associated such as: salmonellosis, shigellosis and acute diarrhoea, for pathogenic bacteria; gastroenteritis, hepatitis A, for pathogenic viruses; giardiasis, hookworm infection, for pathogenic parasites.^[1]

These pollutants need to be eliminated from the water and appropriate measures must be taken for its prevention, control and eradication for the wellbeing of all living organisms and to protect them from various diseases.^[10]

1.1.2. Treatment

Water treatment consists of processing contaminated water to achieve water quality regulations, which have become more rigorous through time and requires specified goals and standards imposed by regulatory agencies and/or local communities.^[12]

Ancient Sanskrit and Greek, in 4000 B.C., focused mainly on methods to improve the aesthetic qualities of drinking water (transparency, taste and odour) such as filtering through charcoal or sand, exposing it to sunlight, boiling and straining. With the evolution in knowledge and science, scientists focused in developing water treatment processes to cover especially the contaminants that are not visible to the naked eye in order to prevent waterborne disease outbreaks.^{[12],[13]}

In 1855, the epidemiologist Dr. John Snow demonstrated that a cholera epidemic in London was a waterborne disease, and, ten years later, Dr. Louis Pasteur developed his germ theory that account for the possibility of microscopic organisms transmit disease through aqueous media.^[13]

At the end of the nineteenth century, while Fuller developed conventional water treatment processes for the removal of contaminants from municipal water supplies like coagulation, flocculation, sedimentation or filtration, Smith advanced with the development of the coliform test to assess the presence of sewage contamination in a water source.^[12]

In the twentieth century, most of the methods developed for water disinfection evolved from physical observations such as the need to reduce water turbidity, to the recognition of the relationship between microorganisms in contaminated water and diseases like typhoid fever or dysentery.^[13]

The exploration of treatment technologies focused on the use of disinfectants like chlorine or ozone to reduce waterborne disease outbreaks was the next important advance. Continuous chlorination uses chlorine releasing chemicals to eliminate germs.^[1]

The implementation of conventional water treatment and chlorine disinfection of surface supplies were crucial to consider most water supplies in developed countries as microbiologically safe by 1940.^[12] However, the chlorination process leaves sufficient free residual chlorine in the water to prevent further contaminations. A drawback of this usage is the fact that chlorine is extremely poisonous and can form by-products through reaction with organic matter (some of them suspected to be carcinogens).^[1]

The application of ozone or ultraviolet (UV) radiation as a final disinfectant is limited. In contrast to what happens when chlorine is used as the disinfectant, these processes do not leave residual disinfectant content in the water, and thus subsequent contamination may occur.^[14]

Treatment technologies such as ion exchange, aeration, activated carbon adsorption and membrane technologies were introduced during the twentieth century in response to more complex treatment goals. The main advantages and drawbacks of these technologies are summarised in Table 1.

Table 1. Advantages and drawbacks of different water treatment process.^{[12],[15],[16]}

Process	Advantages	Drawbacks
Ion exchange	<ul style="list-style-type: none"> - Ability to remove a wide variety of inorganic species. - Removal of hardness responsible ions (calcium and magnesium). 	<ul style="list-style-type: none"> - Expensive to implement at the municipal scale.
Aeration	<ul style="list-style-type: none"> - Air does not need to be purchased. - Aeration ensures that the water is well mixed and remains homogeneous. 	<ul style="list-style-type: none"> - Longer aeration period requires more energy and higher costs. - Temperature sensitive.
Activated carbon adsorption	<ul style="list-style-type: none"> - Organic chemicals can be effectively removed. - High efficiency in VOC removal. - Easy to maintain. 	<ul style="list-style-type: none"> - Risk of spontaneous combustion in the bed. - Component mixes may lead to early malfunction.
Membranes	<ul style="list-style-type: none"> - Continuous rejection of microbiological contaminants by size exclusion. - Membrane could be backwashed, not needing to be disposed after each use. 	<ul style="list-style-type: none"> - Prone to membrane fouling effects which lead to decrease in permeate flux. - High flow rates can damage shear sensitive materials.

Nowadays, the disinfection of water in municipal treatment systems is carried out through both physical processes (boiling, filtration and ultraviolet light) and chemical processes (application of chlorine, chlorine dioxide, monochloramine and ozone).^[14] As all disinfection processes have advantages and limitations, as prior mentioned, a combination between the effectiveness of the process (inactivation of microorganisms), formation of by-products and the guarantee of a residual content throughout the distribution system (health protection) should be pursued.

Since it is predicted the increase, in the long run, of new and more complex contaminants, the number and effectiveness of water treatment techniques are also expected to increase.

1.2. Water Biocontamination

1.2.1. Biofouling

Fouling is an undesirable process in which a surface is inlaid with material from the surrounding environment. When these materials are organisms and their by-products, this process is called biofouling. Biofouling occurs in clean surfaces submerged in aqueous environments (e.g. pipelines, ship hulls, tanks, filters) and also on surfaces, such as countertops, surgical tools and doors.^[17]

Using a surface submerged or in contact with water as a representative example, the biofouling process can be explained as the primary formation of a film (microfouling or slime) which is spontaneous and almost immediately formed by micro-organisms (e.g. bacteria, algae and protozoa). This film promotes the fixation and settlement of macro-organisms such as invertebrates (ex. corals, mussels, barnacles, anemones) and macroscopically visible algae (seaweed).^{[18],[19]} This process is depicted in Figure 1.

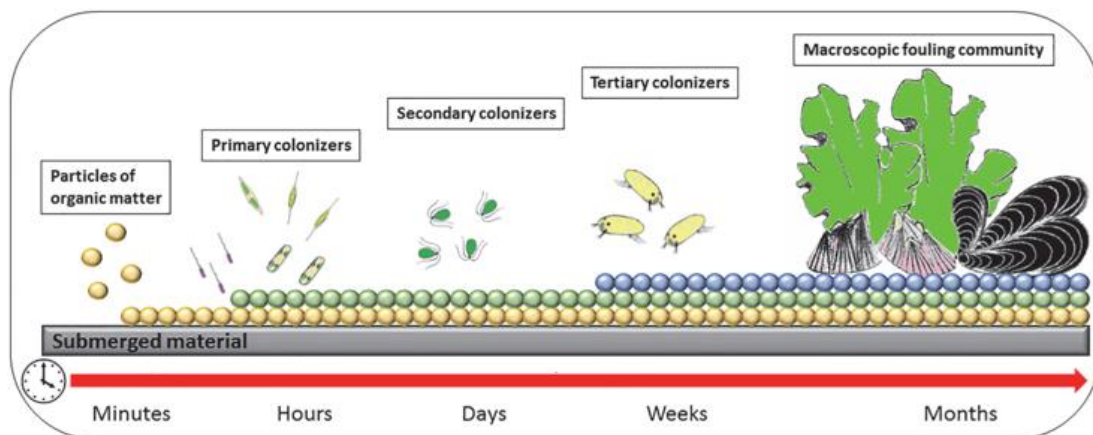


Figure 1. Representative scheme of the marine biofouling process.^[20]

Biofouling is related with environmental and economic losses in a wide range of industrial sectors, such as, water purification systems, desalination, and aquaculture as well as in the maritime industry. Its impact is usually associated with premature deterioration of materials (biocorrosion). In the case of the marine transport sector, the colonization of submerged surfaces of ship hulls, Figure 1, causes several problems like a significantly increase of drag friction, which reduces the ship speed, increases fuel consumption by up to 30-40%, reduces navigation power by up to 86% at cruising speed, implies extensive maintenance and increase the greenhouse gas emissions of CO₂, CO, SO₂ and NO_x.^{[21],[22],[23]}



Figure 2. Biofouling on a ship's hull. Courtesy of Hempel's Marine Paints A/S.^[24]

Biofouling can also cause problems in water distribution and treatment systems (Figure 2). The occurrence of this process leads to water contamination, early deterioration of the equipment and associated systems, which implies more maintenance, temporary stops, and more frequent replacement of equipment of the systems that results in high operational and capital costs.



Figure 3. Biofouling on a cooling water pipe in the ship's system.^[25]

In water supply distribution systems, the most common changes that can occur as the result of the formation and presence of a biofilm are:^[26] i) decrease in residual chlorine and detachment of bacteria from the biofilm which lead to increased bacterial counting; ii) taste and odour changes; iii) reduction of dissolved oxygen content due to the microbial activity in the biofilm; iv) "red water" resulting from the activity of iron bacteria; v) increased "hydraulic roughness" due to higher turbulence that increases mass transfer rates, and thus influences corrosion rates, leaching rates, and detachment of bacteria from the biofilm.

1.2.2. Control and prevention of biofouling

Solutions for biofouling control have been widely explored, including the application of “environmental friendly” strategies as the development of antifouling coatings. This approach has some advantages due to its simplicity, versatility, and efficiency.

Antifouling coatings can be divided into two main categories: biocidal and biocide-free coatings. Biocidal coatings release chemicals (toxic compounds), like copper-based compounds, to avoid settlement or the survival of aquatic organisms. On the other hand, biocide-free coatings rely only on their physical nature.^[27]

Polymeric antifouling coatings are biocidal coatings that incorporate one or more bioactive chemical compounds (biocides) used to inhibit or prevent the adhesion and growth of microorganisms on submerged surfaces or in contact with aqueous media.^[14]

Antibacterial coatings can be based on release strategies (antibacterial agent release) or non-release approaches (contact-killing and anti-adhesion). Their main applications, advantages and limitations are shown in Table 2.^[28]

Table 2. Antibacterial coatings approaches.^[28]

Antibacterial coating	Applications	Advantages	Limitation
Antibacterial Agent Release	Leaching loaded antibacterial compounds over time, killing adhered and adjacent bacteria.	High local antibacterial agent concentration, without exceeding systemic toxicity or ecotoxicity limits.	- Limited reservoirs of antibacterial agents and, therefore reduced life cycle. - Possibility of antimicrobial resistance development.
Contact-Killing	Antimicrobial compounds are covalently bonded to the surface by flexible, hydrophobic polymeric chain.	Avoid the reservoir exhaustion of release-based coatings.	Surfaces contaminated with materials that are attached non-specifically, resulting in their deactivation.
Anti-Adhesion	Surface immobilization of molecules that can resist protein adsorption.	Prevent the initial, rapid, and reversible step of biofilm formation using non-cytotoxic mechanisms.	Have stability issues and are more complex than expected.

The design and synthesis of several coating systems has been attempted by researchers around the world like the use of foul-release silicone (PDMS) or polyurethane (PU) based coatings.^[29] Currently, the use of antifouling silicone-based coatings has proven to be one of the most environmental friendly methods for controlling biofouling events prone to offer smoother surfaces. Nevertheless, the highest antifouling efficacy is still provided by biocidal coatings.

Among those, the choice of an appropriate antifoulant agent rely on their antimicrobial ability, chemical reactivity and toxicity, once it affects coatings effectiveness, polymerization, synthesis and immobilization.^[30]

Econea is a commercial biocide that has been applied as an antifouling agent to combat marine biofouling. Its wide spectrum of action, especially for hard foulants, and relatively short lifetime (about 3 hours in seawater) are important aspects that give to this antifouling agent high potential to replace most toxic antifouling agents.^[31]

Macrocyclic polyamines, in particular cyclam derivatives, have drawn attention in recent years, as antifouling agents. These compounds were used in coating formulations suitable for fresh water and aquatic environments.^[14] However, optimization of their structure/activity relationship as well as verifying its effect in more suitable matrices, such as a polyurethane-based matrix able to provide higher physical-chemical resistance for water treatment systems than conventional silicone-based matrices is still not well explored.

The main objective of this work is to demonstrate that cyclam derived compounds can be incorporated into polyurethane polymeric coatings as an innovative technology for the treatment of biofouling in water treatment and distribution systems.

1.3. Protective Coatings

Since this dissertation aims the incorporation of compounds derived from cyclam in antifouling paints, it is important to make a brief introduction about paints in a general scope, their general characteristics and classification, with a special focus on antimicrobial and antifouling paints.

The use of paints by man dates to the Stone Age, when they began to paint figures on the walls of caves to memorize their lives and for decorative purposes.^[32]

In recent years, the paint technology has undergone changes not only due to the introduction of regulations aimed to protect the environment, health, and safety of population, but also because of cost/benefit ratios. Advance in technology and environmental regulations related to dust particles and abrasive blasting, emission of volatile organic compounds (VOCs) and hazardous materials led to the development of new paints and finishes with less impact on the environment and human health.^{[33],[34]} Currently, paints and similar products have varied uses, such as decoration, improvement of objects aspect and protection of surfaces.^[35]

1.3.1. General characteristics and classification of paints

ISO 4618 defines paint as a “substance composed of solid colouring matter suspended in a liquid medium and applied as a protective or decorative coating to various surfaces, or to canvas or other materials in producing a work of art” and will always be called paint no matter how the coating is cured, how it is applied or what other components it contains.^[36]

They are composed by the combination of two phases: a dry extract (solid part – resins, pigments and additives) and a volatile vehicle (liquid component – solvents and diluents), with different components that interact physically and chemically with each other. Each paint mixture is made according to a certain formulation, so that after applied and cured, it can acquire the desired performance characteristics and physical properties.^{[33],[35]}

Paints can be divided based on their physical form, according to the solvent and depending on their constituents (Table 3) or be classified depending on the nature of the solvent, the nature of the ligand or the intended purpose (Table 4).^{[33],[37]}

Table 3. Paints divided based on their physical form, according to the solvent and depending on their constituents.^[37]

Type of paint	Properties	
Solvent-borne paints	Up to 80% of solid constituents (binders, pigments and additives) dispersed in the organic solvent; dry fast; may contain a wide range of binders; toxic and combustible.	
Water-borne paints	Water as solvent; non-toxic and non-combustible; long drying time.	Based on water-soluble binders
		Based on polymer dispersions (emulsion paints)
High-solids paints (low VOCs paints)	More than 80% of solid constituents (binders, pigments) dispersed in an organic solvent.	
Powder coatings	Obtained by electrodeposition of particles from powdered resin that are attracted by electrostatic force to the substrate surface; no solvent involved; no/low toxic waste; high cost of equipment.	
Radiation curable	Mixture of prepolymers, monomers and additives that cure under ultra-violet radiation; harden fast; no solvents; relatively high cost.	

Table 4. Paints matrices in accordance with their solvent or ligand nature.^[33]

Nature of paint		
Based on the nature of the solvent	Water as solvent	Acrylic or vinyl water paints and water-based enamels.
	Solvent is not water	Powder paints, pasta and acrylic, vinyl, epoxy, and rubber solvent paints.
Based on the nature of the ligand		Acrylic, methacrylic, bituminous, nitrocellulose, polyester, polyurethane, among others.

2. Materials and methods

2.1. General Considerations

Compounds **1**^[38], **2**^[39], **4**^[40], **5**^[41], **6**^[42], **7**^[43], **8**^[44] and **9**^[44] were prepared according to published procedures. Tetraazadodecane and all other reagents and solvents were of commercial grade and used without further purification. Compounds **1** and **6** were done in duplicate and compound **7** in triplicate and thus, the final mass corresponds to the total amount of the compounds obtained.

2.2. Characterization Techniques

Elemental analyses

Elemental analyses for carbon (C), hydrogen (H) and nitrogen (N) were performed in a Fisons CHNS/O analyser Carlo Erba Instruments EA-1108 equipment at the IST Analyses Laboratory.

Fourier Transform Infrared Spectroscopy (FTIR) – ATR-IR

IR spectra were acquired in a Bruker ALPHA II ATR spectrometer with an individual diamond in the range of 400-3800 cm⁻¹ with 4 cm⁻¹ resolution.

Mass Spectroscopy

Mass spectra were obtained using the electrospray ionization technique in an Ion Trap 500-MS, Varian Inc mass spectrometer from the Portuguese mass spectrometry network.

Nuclear Magnetic Resonance Spectroscopy

NMR spectra were recorded, at 296 K, in a Bruker AVANCE II 300 or 400 MHz spectrometers referenced internally to residual proton-solvent (¹H) or solvent (¹³C) resonances and reported relative to tetramethylsilane (0 ppm). ¹⁹F NMR was referenced to external CF₃COOH (-76.55 ppm). HSQC and ¹H-¹H COSY NMR experiments were used to assign all proton and carbon resonances.

Single crystal X-ray diffraction

Crystals of compounds **8**, **10**, **11** and **12** were coated and selected in Fomblin® oil, mounted on a loop and crystallographic data were collected using graphite monochromated Mo-K α radiation ($\lambda = 0.71073 \text{ \AA}$) on a Bruker AXS-KAPPA APEX II diffractometer equipped with a cooling system of Oxford Cryosystem nitrogen. The unit cell parameters were retrieved using the Bruker SMART software and refined using Bruker SAINT in all the observed reflections.^[45] Absorption corrections were applied using SADABS.^[46] The structures were solved by direct methods using SIR97^[47] or SIR2004^[48], and the refinement was done using SHELXL-97.^[49] These programs are part of the WinGX software package version 1.80.05.^[50] The OH groups' hydrogen atoms were

located on the electronic density map. All other hydrogen atoms were inserted into fixed and refined positions on the corresponding carbon atom. The illustrations of the molecular structures were made with ORTEP3 for *Windows*.^[51]

2.3. Synthesis of compounds

Compound 1

Ni(ClO₄)₂·6H₂O (55.18 g, 0.15 mol) was dissolved in 400 mL of distilled water and 28 mL of tetraazadodecane (0.15 mol) were added, whilst stirring. The solution formed was cooled to around 5°C (in an ice bath) and 22 mL of glyoxal at 40% were added (0.48 mol). The reaction mixture was stirred overnight at room temperature. The solution was cooled to 5°C and two equivalents of sodium borohydride (11.12 g, 0.29 mol) were slowly added. The solution was stirred until the foam disappeared and refluxed for 1 hour. The hot solution was then filtered and, after cooling to room temperature, sodium cyanide (29.65 g, 0.60 mol) was added. The mixture was refluxed for 2 hours and thereafter sodium hydroxide (15 g, 0.39 mol) was added. The solvent was evaporated in the rotavapor until formation of a beige paste. The product was extracted with several portions of chloroform. The organic phases were combined and dried with MgSO₄ anhydrous. The solution was filtered, and the solvent evaporated to dryness under reduced pressure, affording the compound as a white solid with 39% yield (23.42 g, 0.12 mol, total duplicates).

¹H NMR (CDCl₃, 400.1 MHz, 296 K): δ (ppm) 2.80 (b, 4H, NH), 2.73 (m, 8H, [C3]CH₂N), 2.66 (m, 8H, [C2]CH₂N), 1.71 (m, 4H, CH₂CH₂CH₂).

Compound 2

Cyclam (2.00 g, 9.98 mmol) was dissolved in 70 mL of dry toluene, 1.82 mL of P(NMe₂)₃ were added (10 mmol) and the reaction mixture was refluxed for two days. The orange solution obtained was filtered under an inert atmosphere of nitrogen while hot. It was allowed to cool down to room temperature and 10 mL of carbon tetrachloride were added. The solvent was evaporated in the vacuum line. A solution of sodium hydroxide (4M) was added until a pH ~ 14. The reaction mixture was extracted with several portions of chloroform, which were combined and dried with MgSO₄ anhydrous. The solvent was evaporated in the rotavapor, without letting it dry, and left to precipitate overnight in the freezer. Since no precipitate was obtained, more solvent was evaporated in the rotavapor and the concentrated solution added dropwise to n-hexane. The brownish paste obtained was purified by flash chromatography using a solution of methanol:chloroform (1:1) as eluent. The compound was obtained with 48% yield (1.17 g, 4.79 mmol).

¹H NMR (CDCl₃, 300.1 MHz, 296 K): δ (ppm) 3.80-3.68 (m, 2H), 3.46 (s, 1H, NH), 3.40-3.27 (m, 2H), 3.12-2.88 (m, 6H), 2.78-2.65 (m, 6H), 1.99-1.59 (m, 4H, CH₂CH₂CH₂). ³¹P NMR (CDCl₃, 121.5 MHz, 296 K): δ (ppm) 26.2 (2, P=O)

Compound 3

Compound **2** (0.84 g, 3.44 mmol) was dissolved in 30 ml of acetonitrile and potassium carbonate (0.71 g, 1.5 equiv.) was added. Aryl bromide (0.90 g) was dissolved in 10 mL of acetonitrile and refluxed for one day. An aqueous solution of KHCO_3 was added to promote phase separation. The compound was extracted with several portions of chloroform. The organic phases were combined, dried with MgSO_4 anhydrous, and evaporated to dryness in the rotavapor. The product was dissolved in a mixture of toluene and chloroform and filtered while still hot. The solution was concentrated by solvent evaporation in the vacuum line until precipitate formation began to occur and left overnight in the freezer. The solution was filtered affording the compound as a white solid with 29% yield (0.40 g, 0.99 mmol).

^1H NMR (CDCl_3 , 300.1 MHz, 296 K): δ (ppm) 7.67 (d, $^3J_{\text{H-H}} = 8$ Hz, 2H, *o*-Ph), 7.58 (d, $^3J_{\text{H-H}} = 8$ Hz, 2H, *m*-Ph), 7.92-7.87 (overlapping, total 2H, 1H, PhCH_2N and 1H, $[\text{C}3]\text{CH}_2\text{N}$), 3.54 (m, 1H, $[\text{C}2]\text{CH}_2\text{N}$), 3.40-3.27 (overlapping, total 4H, 1H, PhCH_2N , 2H, $[\text{C}3]\text{CH}_2\text{N}$ and 1H, $[\text{C}2]\text{CH}_2\text{N}$), 3.13 (m, 1H, $[\text{C}2]\text{CH}_2\text{N}$), 3.10-2.97 (overlapping, 3H, $[\text{C}3]\text{CH}_2\text{N}$), 2.92 (m, 1H, $[\text{C}3]\text{CH}_2\text{N}$), 2.76-2.29 (overlapping, total 5H, 1H, $[\text{C}3]\text{CH}_2\text{N}$ and 4H, $[\text{C}2]\text{CH}_2\text{N}$), 1.89-1.59 (m, 4H, $\text{CH}_2\text{CH}_2\text{CH}_2$). ^{19}F NMR (CDCl_3 , 282.4 MHz, 296 K): δ (ppm) -62.4 (s, CF_3). ^{31}P NMR (CDCl_3 , 121.5 MHz, 296 K): δ (ppm) 25.3 (s, $\text{P}=\text{O}$). ^{13}C $\{^1\text{H}\}$ NMR (CDCl_3 , 75.5 MHz, 296 K): δ (ppm) 144.0 (*i*-Ph), 129.24 (*o*-Ph), 129.2 ($^2J_{\text{H-H}} = 29$ Hz, *p*-Ph), 125.4 ($^3J_{\text{H-H}} = 4$ Hz, *m*-Ph), 124.4 ($^1J_{\text{H-H}} = 272$ Hz, CF_3), 58.26 (PhCH_2N), 53.05 (2, $[\text{C}2]\text{CH}_2\text{N}$), 51.9 ($J_{\text{C-P}} = 2$ Hz, $[\text{C}2]\text{CH}_2\text{N}$), 45.9 ($J_{\text{C-P}} = 16$ Hz, $[\text{C}2]\text{CH}_2\text{N}$), 44.6 ($J_{\text{C-P}} = 14$ Hz, $[\text{C}3]\text{CH}_2\text{N}$), 42.4 ($[\text{C}3]\text{CH}_2\text{N}$), 42.0 ($[\text{C}3]\text{CH}_2\text{N}$), 41.1 ($J_{\text{C-P}} = 4$ Hz, $[\text{C}3]\text{CH}_2\text{N}$), 26.6-22.2 ($\text{CH}_2\text{CH}_2\text{CH}_2$).

ATR-IR (cm^{-1}): 1112 and 1064 ($\nu_{\text{C-F}}$), 1219 ($\nu_{\text{P=O}}$).

Anal. calcd for $\text{C}_{18}\text{H}_{26}\text{F}_3\text{N}_4\text{OP} \cdot 1/2\text{H}_2\text{O}$: C, 52.55; H, 6.62; N, 13.62. Found: C, 52.39; H, 6.62; N, 13.72.

Compound 4

Compound **1** (1.01 g, 5.04 mmol) was dissolved in 200 mL of dichloromethane (dried with molecular sieves). Under an inert atmosphere of nitrogen, 4 mL of triethylamine and a solution of Boc_2O (1.97 g, 9.03 mmol) in 60 mL of dichloromethane (dried with molecular sieves) was added dropwise. The mixture was cooled at -15°C and another portion of Boc was added (1.39 g, 6.37 mmol). After stirring overnight at room temperature, a saturated solution of sodium carbonate was added. The organic phases were combined, dried with MgSO_4 anhydrous, and evaporated to dryness affording a product with 95% yield (2.37 g, 4.74 mmol).

^1H NMR (CDCl_3 , 400.1 MHz, 296 K): δ (ppm) 3.36-3.31 (overlapping, 16H, $[\text{C}3]\text{CH}_2\text{N}$ and $[\text{C}2]\text{CH}_2\text{N}$), 1.75-1.70 (m, 4H, $\text{CH}_2\text{CH}_2\text{CH}_2$), 1.45 (s, 27H, Boc), 1.26 (s, 1H, NH).

Compound 5

Compound **2** (6.01 g, 0.03 mol) was dissolved in the smallest volume of water. After complete dissolution, an ice bath was used to cool the solution and 6 mL of formaldehyde were added. The reaction mixture was left stirring for 2 hours in the ice bath and then overnight, at room temperature. The precipitate was filtered off and dried in vacuo. The compound was obtained as a white solid with 98% yield (6.60 g, 0.03 mol).

^1H NMR (CDCl_3 , 400.1 MHz, 296 K): δ (ppm) 5.62-5.59 (d, 2H, NCH_2N), 3.35-3.33 (m, 4H, $[\text{C}2]\text{CH}_2\text{N}$), 3.10-3.07 (d, 2H, NCH_2N), 3.03-3.00 (m, 4H, $[\text{C}3]\text{CH}_2\text{N}$), 2.83-2.77 (td, 4H, $[\text{C}3]\text{CH}_2\text{N}$), 2.58-2.55 (s, 4H, $[\text{C}2]\text{CH}_2\text{N}$), 2.44 (m, 2H, $\text{CH}_2\text{CH}_2\text{CH}_2$), 1.39-1.36 (m, 2H, $\text{CH}_2\text{CH}_2\text{CH}_2$).

Compound 6

A solution of 4-(trifluoromethyl)benzyl bromide (4.35 g, 18.20 mmol), done in smallest volume of acetonitrile, was added to a very concentrated solution of compound **5** (2.00 g, 8.92 mmol). The solution was filtered, and the precipitate obtained was collected and dried in vacuum. The product was obtained as a white solid with 98% yield (12.27 g, 0.02 mol, total duplicates).

^{19}F NMR (CDCl_3 , 376.5 MHz, 296 K): δ (ppm) -60.3 (s, CF_3). The fast hydrolysis of the product in D_2O hampered its full characterization by NMR.

Compound 7

The procedure was performed in triplicate using 8.40 g of compound **6** (11.96 mmol) in total. In each flask, the compound was dissolved in 200 mL of distilled water and 400 mL of a sodium hydroxide (3M) solution was added. The reaction mixture was stirred overnight. The compound was extracted with several portions of dichloromethane, the organic phases were combined and dried with MgSO_4 anhydrous. After filtration, the solvent was evaporated to dryness in the rotavapor affording a beige oil, which was transformed into a white solid by repeating freeze/vacuum/thaw cycles. The product was obtained with 64% yield (3.99 g, 7.66 mmol, total).

^1H NMR (CDCl_3 , 300.1 MHz, 296 K): δ (ppm) 7.54 (d, $^3J_{\text{H-H}} = 8$ Hz, 4H, *m*-Ph), 7.42 (d, $^3J_{\text{H-H}} = 8$ Hz, 4H, *o*-Ph), 3.75 (s, 4H, PhCH_2N), 2.77-2.53 (overlapping, total 18H, 8H, $[\text{C}2]\text{CH}_2\text{N}$ and 8H, $[\text{C}3]\text{CH}_2\text{N}$ and b, 2H, *NH*), 1.87 (m, 2H, $\text{CH}_2\text{CH}_2\text{CH}_2$). ^{19}F NMR (CDCl_3 , 282.4 MHz, 296 K): δ (ppm) -62.5 (s, CF_3).

Compound 8

Compound **7** (3.05 g, 5.76 mmol) was dissolved in 150 mL of methanol and 2.20 mL of methyl acrylate were added. After refluxing for 4 hours, the reaction mixture was cooled in the refrigerator and placed in the freezer overnight. The precipitate formed was filtered off and washed with cold

methanol. A second crop was obtained by freezing the filtered solution after concentration. The compound was isolated with a total 74% yield (2.96 g, 4.27 mmol).

^1H NMR (CDCl_3 , 300.1 MHz, 296 K): δ (ppm) 7.58 (d, $^3J_{\text{H-H}} = 8$ Hz, 4H, *m*-Ph), 7.48 (d, $^3J_{\text{H-H}} = 8$ Hz, 4H, *o*-Ph), 3.59 (overlapping, total 10H, 4H, PhCH_2N and 6H, OCH_3), 2.69 (t, $^3J_{\text{H-H}} = 7$ Hz, 4H, $\beta\text{-CH}_2$), 2.59 (m, 8H, $[\text{C}2]\text{CH}_2\text{N}$), 2.50 (m, 8H, $[\text{C}3]\text{CH}_2\text{N}$), 2.37 (t, $^3J_{\text{H-H}} = 7$ Hz, 4H, $\alpha\text{-CH}_2$), 1.69-1.65 (m, 4H, $\text{CH}_2\text{CH}_2\text{CH}_2$). ^{19}F NMR (CDCl_3 , 282.4 MHz, 296 K): δ (ppm) -62.3 (s, CF_3).

Compound 9

Compound **8** (2.92 g, 4.21 mmol) was dissolved in THF (dried with molecular sieves) and added dropwise to a THF suspension of LiAlH_4 (1.18 g, 7.4 equiv.). After refluxing overnight, the reaction mixture was left to cool at room temperature and an aqueous solution of sodium tartrate (10%), and sodium hydroxide (5%) was added dropwise. The product was extracted with several portions of diethyl ether. The organic phases were combined and dried with MgSO_4 anhydrous. The solution was filtered, and the solvent evaporated to dryness affording the compound as a white powder with 90% yield (2.36 g, 3.78 mmol).

^1H NMR (CDCl_3 , 300.1 MHz, 296 K): δ (ppm) 7.58 (d, $^3J_{\text{H-H}} = 8$ Hz, 4H, *m*-Ph), 7.48 (d, $^3J_{\text{H-H}} = 8$ Hz, 4H, *o*-Ph), 5.45 (s, 2H, OH), 3.73-3.66 (overlapping, total 8H, s, 4H, PhCH_2N and t, $^3J_{\text{H-H}} = 6$ Hz, 4H, $\gamma\text{-CH}_2$), 2.51-2.30 (overlapping, total 20H, 4H, $[\text{C}3]\text{CH}_2\text{N}$ and 8H, $[\text{C}2]\text{CH}_2\text{N}$ and m, 4H, $[\text{C}3]\text{CH}_2\text{N}$ and t, $J_{\text{H-H}} = 6$ Hz, 4H, $\alpha\text{-CH}_2$), 1.85 (m, 4H, $\text{CH}_2\text{CH}_2\text{CH}_2$), 1.60 (t, $^3J_{\text{H-H}} = 6$ Hz, 4H, $\beta\text{-CH}_2$). ^{19}F NMR (CDCl_3 , 282.4 MHz, 296 K): δ (ppm) -62.4 (s, CF_3).

Compound 10

Compound **7** (0.60 g, 1.15 mmol) was dissolved in 80 mL of acetonitrile. Three equivalents of both ethyl bromoacetate (0.40 mL) and potassium carbonate (0.48 g) were added, and the mixture was refluxed overnight. Water was added to promote phase separation and the product was extracted with several portions of chloroform. The organic phases were combined, dried with MgSO_4 anhydrous, and evaporated to dryness affording a 98% yield (0.78 g, 1.23 mmol).

^1H NMR (CDCl_3 , 400.1 MHz, 296 K): δ (ppm) 7.55 (d, $^3J_{\text{H-H}} = 8$ Hz, 4H, *m*-Ph), 7.47 (d, $^3J_{\text{H-H}} = 8$ Hz, 4H, *o*-Ph), 4.13-4.04 (m, 4H, CH_2O), 3.59 (s, 4H, PhCH_2N), 3.23 (s, 4H, OCH_2N), 2.76-2.56 (overlapping, 14H, $[\text{C}3]\text{CH}_2\text{N}$ and $[\text{C}2]\text{CH}_2\text{N}$), 1.69-1.67 (m, 4H, $\text{CH}_2\text{CH}_2\text{CH}_2$), 1.18-1.16 (t, 6H, $\text{CH}_3\text{CH}_2\text{O}$). ^{19}F NMR (CDCl_3 , 376.5 MHz, 296 K): δ (ppm) -62.4 (s, CF_3). ^{13}C $\{^1\text{H}\}$ NMR (CDCl_3 , 100.6 MHz, 296 K): δ (ppm) 171.62 (*i*-Ph), 129.26 (*o*-Ph), 125.20 (*m*-Ph), 60.29 (CH_2O), 55.53 (PhCH_2N and OCH_2N), 51.70-51.05 (overlapping, $[\text{C}3]\text{CH}_2\text{N}$ and $[\text{C}2]\text{CH}_2\text{N}$), 24.85 ($\text{CH}_2\text{CH}_2\text{CH}_2$), 14.35 ($\text{CH}_3\text{CH}_2\text{O}$).

Anal. calcd for $\text{C}_{34}\text{H}_{46}\text{F}_6\text{N}_4\text{O}_4 \cdot 3/2\text{H}_2\text{O}$: C, 57.05; H, 6.90; N, 7.83. Found: C, 56.99; H, 6.79; N, 7.80.

Compound 11

Compound **11** was synthesized as described for compound **9**.

Herein, compound **10** (0.98 g, 1.41 mmol) was dissolved in dry THF and added dropwise to a THF suspension of LiAlH₄ (0.40 g, 7.4 equiv.). The mixture was refluxed overnight. After cooling to room temperature, an aqueous solution of sodium tartrate (10%) and sodium hydroxide (5%) was added dropwise. The product was extracted with several portions of diethyl ether. The organic phases were combined and dried with MgSO₄ anhydrous. The solution was filtered, and the solvent evaporated to dryness. The crude was washed with n-hexane and few drops of diethyl ether were added to obtain the product as a white powder with 20% yield (0.17 g, 0.28 mmol).

¹H NMR (CDCl₃, 300.1 MHz, 296 K): δ (ppm) 7.58 (d, ³J_{H-H} = 9 Hz, 4H, *m*-Ph), 7.51 (d, ³J_{H-H} = 6 Hz, 4H, *o*-Ph), 4.73 (s, 2H, OH), 3.65 (s, 4H, PhCH₂N), 3.49 (t, ³J_{H-H} = 2 Hz, 4H, β-CH₂), (overlapping, 16H, [C3]CH₂N and [C2]CH₂N), 2.31 (t, ³J_{H-H} = 2 Hz, 4H, α-CH₂), 1.77-1.75 (m, 4H, CH₂CH₂CH₂). ¹⁹F NMR (CDCl₃, 282.4 MHz, 296 K): δ (ppm) -62.4 (s, CF₃). ¹³C {¹H} NMR (CDCl₃, 75.5 MHz, 296 K): δ (ppm) 142.09 (*i*-Ph), 130.14 (*o*-Ph), 129.6 (³J_{H-H} = 32 Hz, *p*-Ph), 125.21 (³J_{H-H} = 4 Hz, *m*-Ph), 124.0 (³J_{H-H} = 272 Hz, CF₃), 59.85 (β-CH₂), 59.30 (PhCH₂N), 54.17 (α-CH₂), 53.51-48.92 (overlapping, [C3]CH₂N and [C2]CH₂N), 25.08 (CH₂CH₂CH₂).

Anal. calcd for C₃₀H₄₂F₆N₄O₄: C, 59.59; H, 7.00; N, 9.27. Found: C, 59.28; H, 7.55; N, 9.22.

Compound 12

Compound **7** (0.47 g, 0.90 mmol) was dissolved in 15 mL of acetonitrile and 0.30 mL of acrylonitrile were added. After refluxing the reaction mixture overnight, the suspension rendered a yellow solution which was evaporated to dryness. After an analysis of the NMR spectrum, it was found that we still had the initial reagent present, and the flask was left overnight in the freezer with the intention of precipitate formation. Since the aforementioned did not occur, the compound was precipitated in pentane, the flask was again left in the freezer overnight and evaporated to dryness, affording a 53% yield (0.30 g, 0.48 mmol).

¹H NMR (CDCl₃, 300.1 MHz, 296 K): δ (ppm) 7.58 (d, ³J_{H-H} = 7 Hz, 4H, *m*-Ph), 7.47 (d, ³J_{H-H} = 7 Hz, 4H, *o*-Ph), 3.59 (s, 4H, PhCH₂N), 3.00-2.50 (overlapping, 20H total, 4H, α-CH₂, 4H, β-CH₂ and 12H, [C3]CH₂N or [C2]CH₂N), 2.34 (m, 4H, [C3]CH₂N or [C2]CH₂N), 1.70 (m, 4H, CH₂CH₂CH₂). ¹⁹F NMR (CDCl₃, 282.4 MHz, 296 K): δ (ppm) -63.3 (s, CF₃).

Reaction of **7** and **9** with 4,4'-MDI^[21]

The selected compound was dissolved in dried THF in a content ranging from 5 to 10 wt. % and added dropwise to 4,4'-methylenediphenyldiisocyanate with an isocyanate content (NCO) of 32.9 ± 0.7%. For a content of 5 wt. % a 1:0.6 ratio (cyclam:isocyanate) was used and for a content of 10 wt. % the ratio applied was 1:1.4. The reaction was performed under inert atmosphere conditions (357 mbar) and continuous stirring (300 rpm) at 40 ± 5 °C for about 1 hour per gram of

compound. The precipitate formed was filtered, purified, and dried by solvent evaporation under reduced pressure.

2.4. Incorporation of cyclam compounds in polymeric coatings

Several formulations were prepared following an iterative process, in which the contents of bioactive compound, polymeric base, curing agent (CA) and solvent were varied. The polymeric matrix used was chosen based on paints suitable for aqueous media. It was used a polyurethane (PU, Ref. F0038), kindly supplied by Hempel S/A, Denmark, composed by two components (base + curing agent). The incorporation of the compounds in the coating began with the selection of the most suitable solvent, in terms of compatibility, both with the compound and coating formulation components. Thus, compounds were dissolved in N-methyl-2-pyrrolidone (Sigma-Aldrich, pa), and the base was added. The addition of the curing agent was performed in accordance with the base/CA proportion recommended by the supplier. This iterative optimization process involved the painting of four polyvinyl chloride (PVC) plaques (2x2 cm) for each formulation (see Figure 4) to evaluate the curing and the final properties of the obtained film.

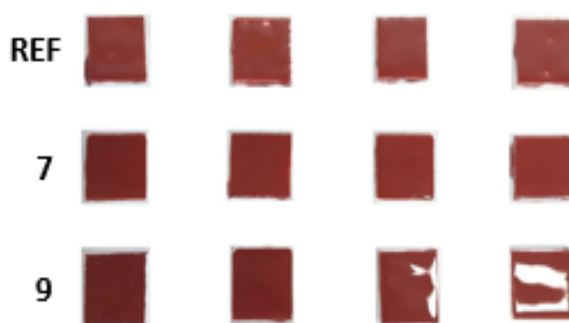


Figure 4. PVC plaques coated with formulations containing a control coated reference plaque without any compound (REF) and the compounds **7** and **9**.

2.5. Evaluation of antimicrobial activity of coatings containing cyclam derived compounds

Antimicrobial activity assessments were performed, in coated Petri dishes, for coatings containing the most promising cyclam derived compounds **7**, **9** and **11** in a polyurethane-based marine coating (PU, Ref. F0038 by Hempel A/S) and the control coated reference (pristine PU coating), against gram-positive Methicillin-resistant *Staphylococcus aureus* (MRSA, ATCC 33591)^[21] and gram negative *Escherichia coli* (*E. coli*, ATCC 25922) strains.

In previous studies, the minimum inhibitory concentrations (MIC) of compounds **7**, **9** and **11** were determined against MRSA and *E. coli*. Compound **7** revealed the highest activity as a chloride or acetate salt against both bacteria.^{[14],[52]}

2.6. Leaching tests

Leaching tests were performed according to modified published procedures[53] and to the international standards ISO 15181-1 (2007) and OECD standard 313 (2007).

Coated acrylic panels (5x10 cm) were immersed in 500 mL of distilled water, under continuous stirring (200 rpm), for a minimum period of 45 days (Figure 5). The pH and temperature were monitored over time.



Figure 5. Leaching test of panels coated with the optimised formulations containing the compounds **7**, **9** and **11** and control coated reference panel submerged in distilled water.

After 45 days of submersion, the obtained leaching waters were analysed by High Performance Liquid Chromatography coupled to Mass Spectrometry (HPLC-MS), in a LCQ Fleet mass spectrometer with and ESI source (Thermo Scientific) interfaced with an HPLC-DAD (Varian) at the Mass Spectrometry Facility (IST-NODE@CQE). The conditions of the leaching tests did not vary significantly over the test time, the pH remained at 6 and the temperature ranged from 21 to 16 °C.

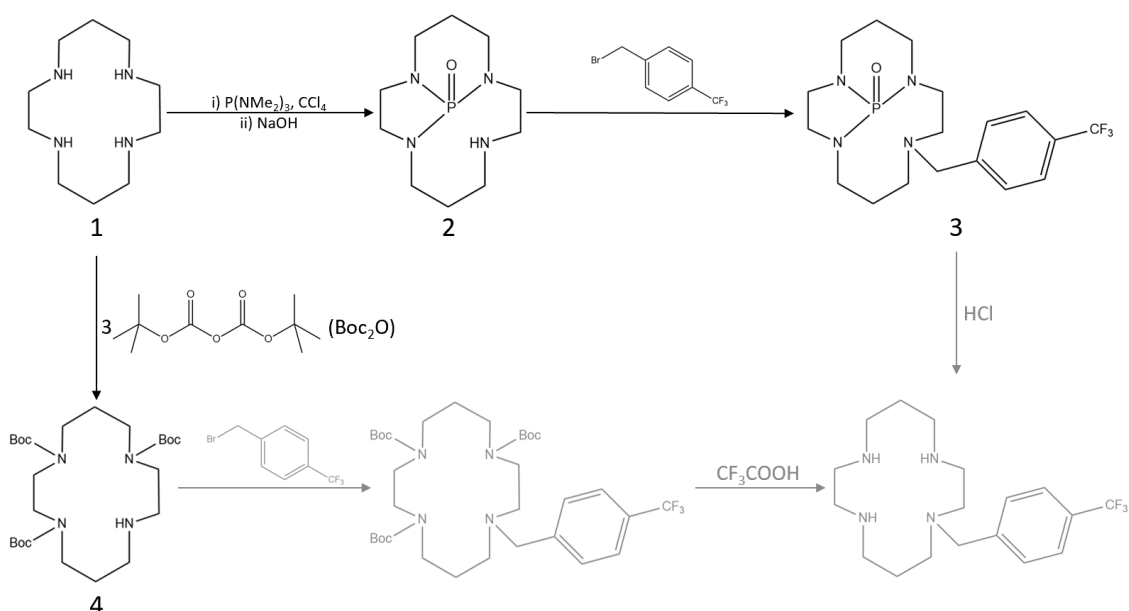
3. Results and Discussion

3.1. Synthesis of cyclam derivatives

The number and/or the chemical nature of the pendant arms of the cyclam ring is known to have a direct effect on the antimicrobial activity of this family of compounds. In this work, the N-substitution of the cyclam ring was carried out following different procedures.

3.1.1. Synthesis of *mono*-substituted cyclam derivatives

Carrying out the *mono*-substitution of cyclam requires the protection of three of the four nitrogen atoms of the macrocycle to selectively functionalize only one of them. Thus, protection was attempted following two different procedures: a) using *tert*-butoxycarbonyl (Boc) groups by reaction of cyclam with 3 equiv. of *di-tert*-butyl dicarbonate (Boc₂O) and b) by transamination of tris(dimethylamino)phosphine with cyclam (see Scheme 1).^[53]



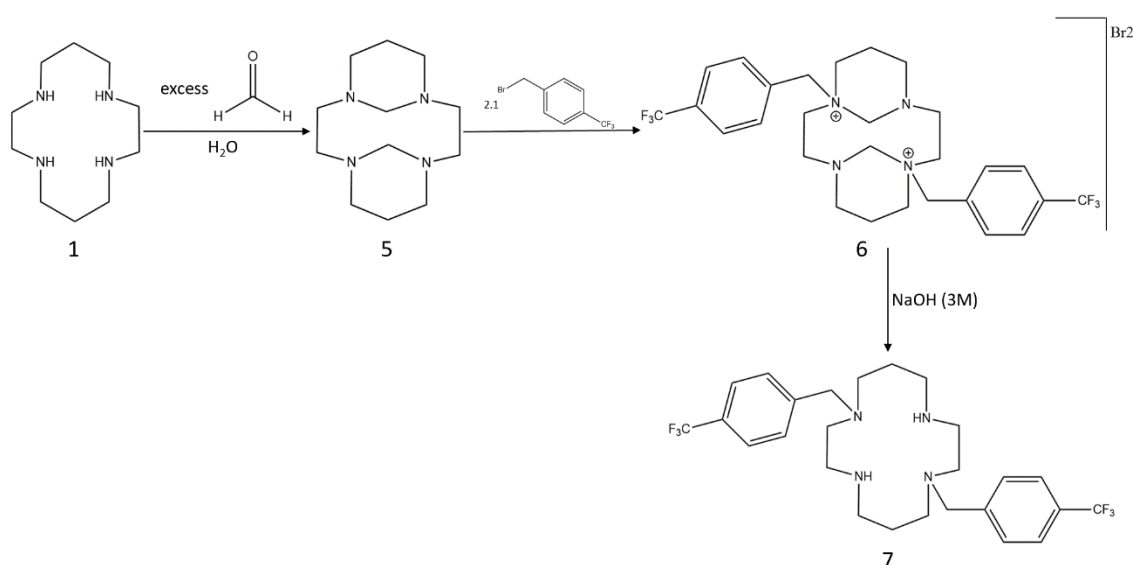
Scheme 1. Reaction scheme of the synthesis of *mono*-substituted cyclam derivative. (Compounds in grey were not successfully achieved)

The reaction of H(Boc)₃Cyclam, **4**, with 4-(trifluoromethyl)benzyl bromide did not lead to the formation of the desired *mono*-substituted compound (4-CF₃PhCH₂)(Boc)₃Cyclam as a mixture of reagents was observed in the ¹H NMR spectrum.

The reaction of cyclam with tris(dimethylamino)phosphine led to transamination with formation of H(P=O)Cyclam, **2**. Compound (4-CF₃PhCH₂)(P=O)Cyclam, **3**, was obtained in 29% yield through the reaction of compound **2** with 4-(trifluoromethyl)benzyl bromide. An attempt was made to remove the P=O group from the cyclam ring, but, probably due to the sensitivity of the intermediate compounds, the isolation of the *mono*-substituted product was not successfully achieved.

3.1.2. Synthesis of *trans*-di-substituted cyclam derivatives

The reaction of cyclam with two equivalents of an alkyl or aryl halide yields a mixture of mono-, di-, tri- and even tetra-substituted derivatives.^[41] To obtain exclusively the di-substituted derivative, the protection of two nitrogen atoms is needed. The procedure followed to obtain the *trans*-di-substituted cyclam $\text{H}_2(4\text{-CF}_3\text{PhCH}_2)_2\text{Cyclam}$, **7**, is shown in Scheme 2. Cyclam, **1**, was reacted with an excess of formaldehyde to give a tricyclic compound **5**, which displays two methylene cross-bridges between adjacent nitrogen atoms. These cross-bridges allow the nucleophilic attack in the nitrogen atoms placed in *trans* position because these atoms are the less sterically hindered and have the electron lone pairs pointing out of the macrocycle backbone. Thus, reacting compound **5** with 4-(trifluoromethyl)benzyl bromide led to the formation of the cyclam salt **6** that was converted into the desired *trans*-di-substituted cyclam through hydrolysis in basic medium.



Scheme 2. Reaction scheme of the synthesis of *trans*-di-substituted cyclam derivative.

The ^1H NMR spectrum of compound **7** represented in Figure 6 reveals the typical pattern for a *trans*-di-substituted macrocycle. The *ortho* and *meta* protons of the $4\text{-CF}_3\text{PhCH}_2$ groups appear as doublets in the aromatic region (7.55-7.41 ppm) and the proton of the CH_2 group of the pendant arm of the cyclam ring show up as a singlet at 3.75 ppm. The protons of the CH_2 groups of the macrocyclic chain are observed between 2.77 and 1.87 ppm.

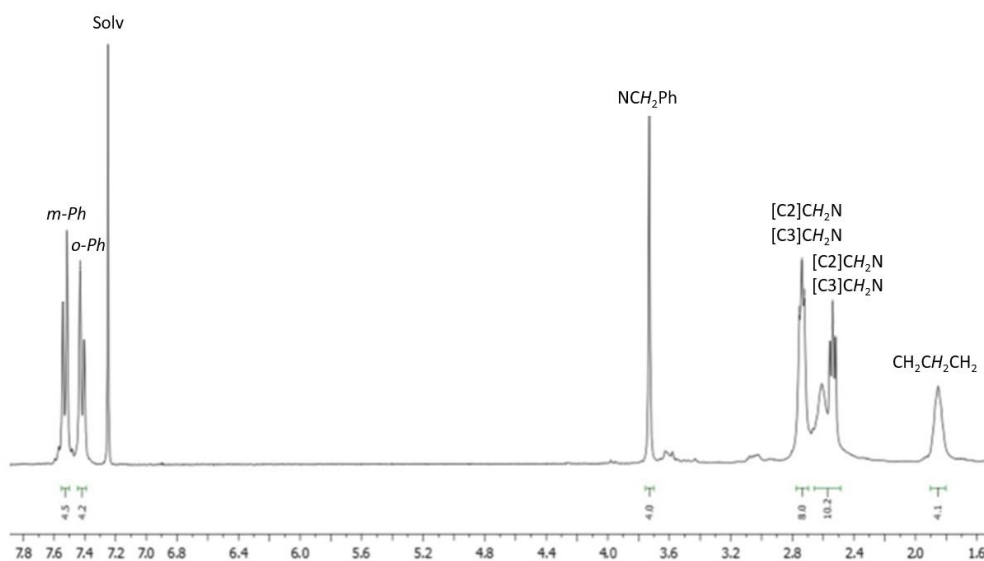


Figure 6. ^1H NMR spectrum of **7** in CDCl_3 at 296K.

3.1.3. Synthesis of *trans*-di-di-substituted cyclam derivatives

The remaining secondary amines of the *trans*-di-substituted cyclam can be further functionalized leading to the formation of *trans*-di-di-substituted cyclam derivatives.

The incorporation of an additional pendant arm with an ester functional group was achieved by reaction of **7** with methyl acrylate leading to compound **8**, as shown in Scheme 3. The reaction of **7** with ethyl chloroacetate or ethyl bromoacetate also led to the formation of an ester functionalized cyclam, **10**. Although the desired product was obtained using both reagents, the reaction of **7** with ethyl bromoacetate led to a higher yield (98%). This observation might be due to bromide being a better leaving group than chlorine. It is also important to mention that to achieve full conversion of compound **7** into **10** a two-step procedure using 2+2 equiv. must be followed when using ethyl chloroacetate (yield of 35%).

Crystals of **8** and **10** suitable for single crystal X-ray diffraction were obtained by slow evaporation of a chloroform solution. Both compounds crystallized in the triclinic P-1 space group with half molecule in the asymmetric unit. Crystallographic and experimental details of data collection and crystal structure determinations are presented in Tables A1 and Table A2 (in Annex) for crystal **8** and **10**, respectively. The solid-state molecular structures of **8** and **10** reveal that the $^4\text{-CF}_3\text{PhCH}_2$ and pendant arms containing the ester groups are in mutually *trans* positions (Figures 7 and 8). All distances and angles agree with the values reported in the literature.^[54]

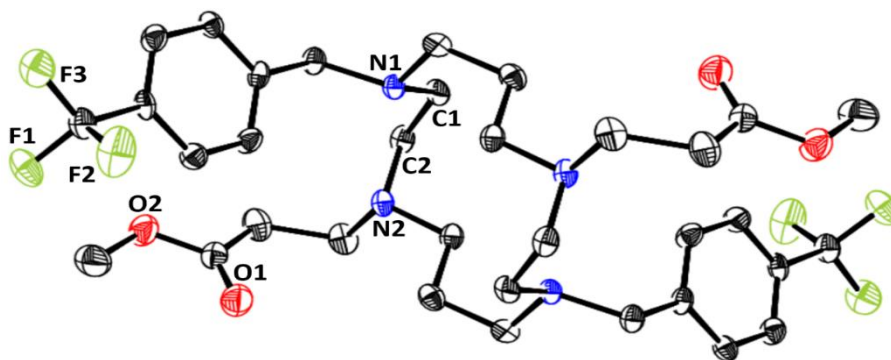


Figure 7. ORTEP diagram of (MeO(O)CCH₂CH₂)₂(⁴-CF₃PhCH₂)₂Cyclam, **8**, showing thermal ellipsoids at 40% probability level. Selected hydrogen atoms are omitted for clarity.

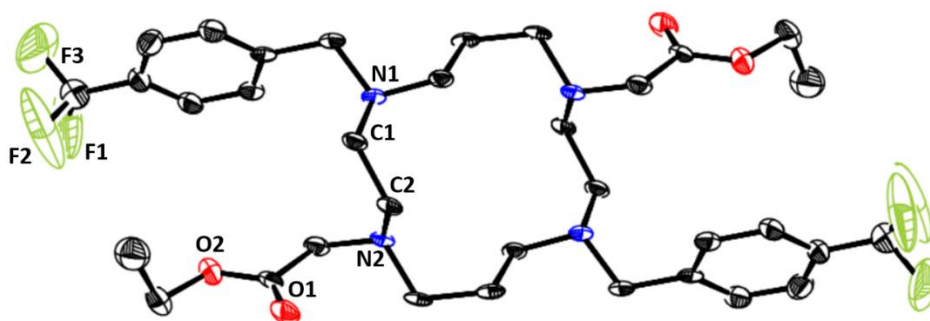
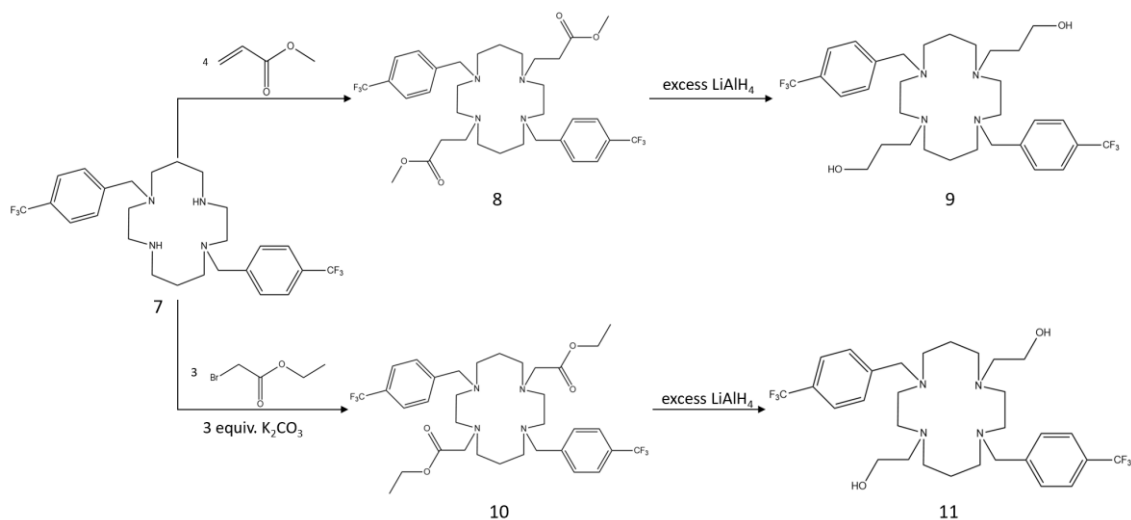


Figure 8. ORTEP diagram of (EtO(O)CCH₂CH₂)₂(⁴-CF₃PhCH₂)₂Cyclam, **10**, showing thermal ellipsoids at 40% probability level. Selected hydrogen atoms are omitted for clarity.

Upon reduction with LiAlH₄, the ester function of the pendant arms of compounds **8** and **10** was converted in alcohol leading to the formation of **9** and **11**, respectively. The overall pathway for the synthesis of compounds **9** and **11** are shown in Scheme 3.



Scheme 3. Reaction scheme of the synthesis of *trans*-di-di-substituted cyclam derivative.

The NMR spectra of both **9** and **11** are similar to the ones presented by their precursors as the symmetry of the molecule remains the same despite the presence of new pending arms attached to the macrocycle. The NMR spectra of **9** and **11** are shown in Figure 9 and 10, respectively.

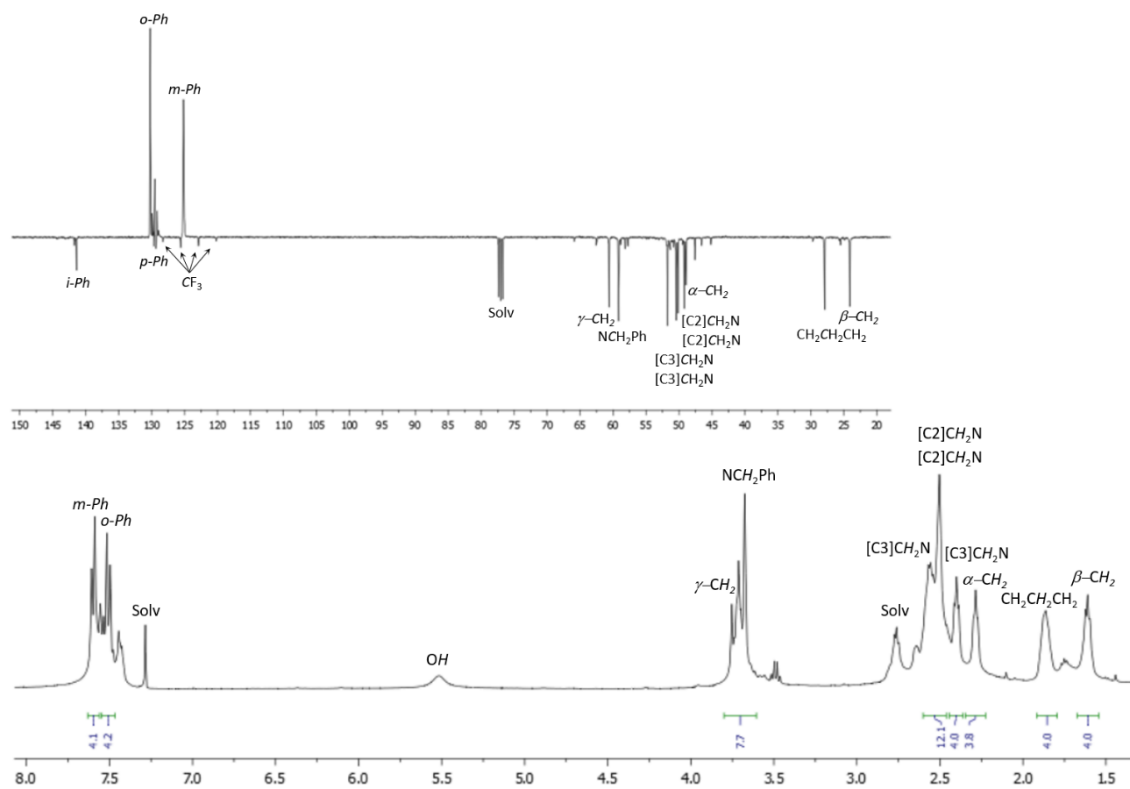


Figure 9. ^1H and $^{13}\text{C}\{^1\text{H}\}$ NMR spectra of **9** in CDCl_3 at 296K.

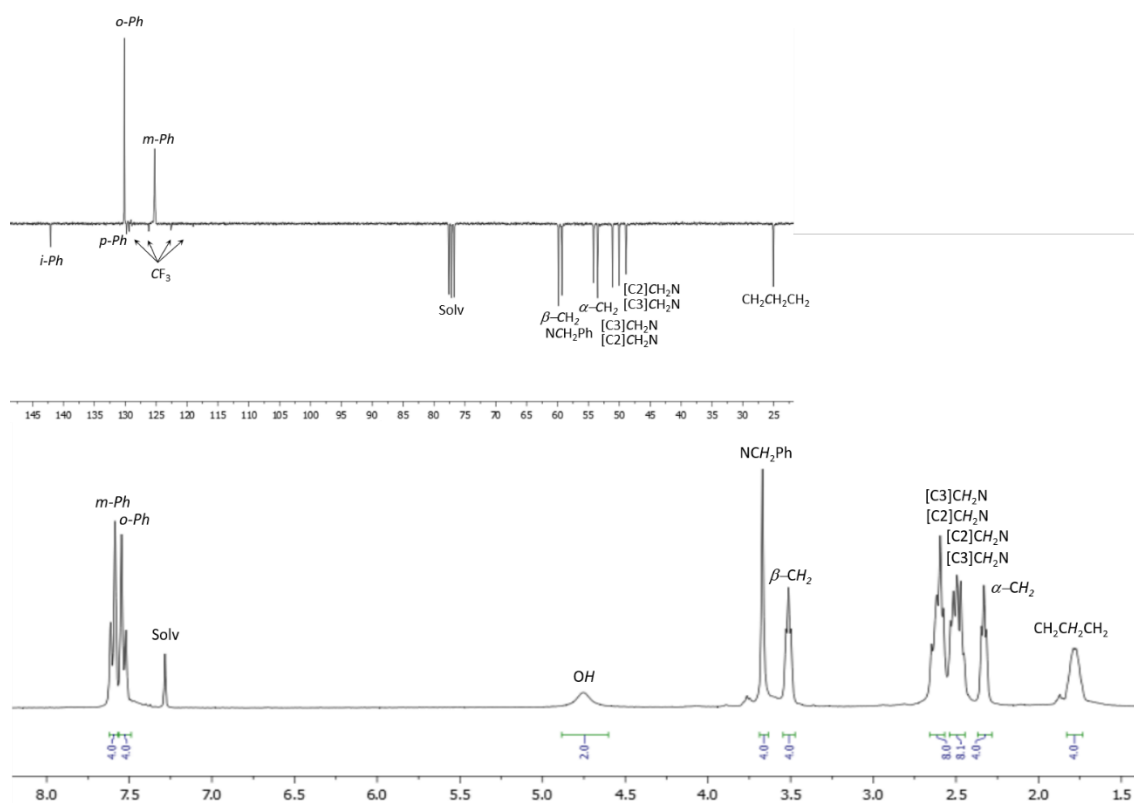


Figure 10. ^1H and $^{13}\text{C}\{^1\text{H}\}$ NMR spectra of **11** in CDCl_3 at 296K.

Crystals of **11** suitable for single crystal X-ray diffraction were obtained by slow evaporation of a chloroform solution. Compound **11** crystallized in the triclinic P-1 space group with half molecule in the asymmetric unit. Crystallographic and experimental details of data collection and crystal structure determinations are presented in Table A3 (in Annex). The solid-state molecular structure of **11** reveals that the $^4\text{-CF}_3\text{PhCH}_2$ and $\text{CH}_2\text{CH}_2\text{OH}$ pendant arms are in mutually *trans* positions are located at opposite sides of the macrocyclic ring (see Figure 11). The structural arrangement of the macrocycle framework is determined by intramolecular hydrogen bonds ($\text{O-H}\cdots\text{N}$) with 2.16(4) Å that form two 8-membered heterocycles. This structure is identical to the one already reported for **9**.^[44]

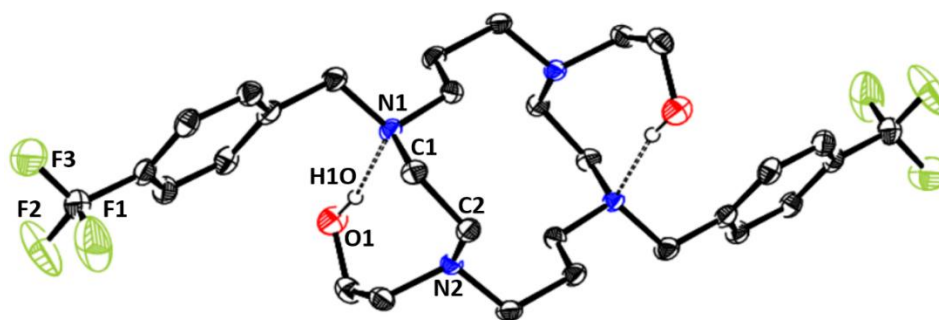
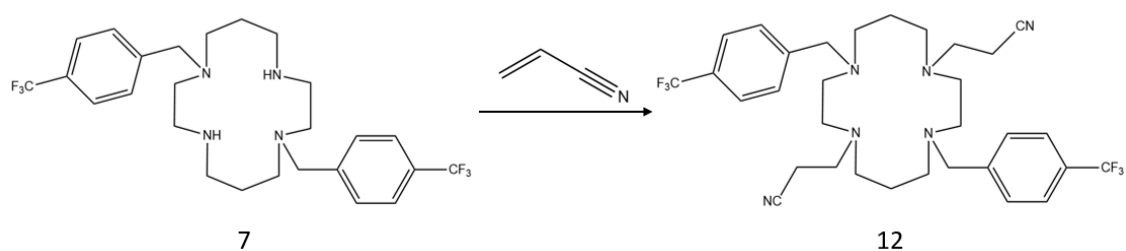


Figure 11. ORTEP diagram of $(\text{HOCH}_2\text{CH}_2)_2(^4\text{-CF}_3\text{PhCH}_2)_2\text{Cyclam}$, **11**, showing thermal ellipsoids at 40% probability level. Selected hydrogen atoms are omitted for clarity. Dashed lines represent hydrogen bonds.

Attempts to synthesize cyclam derivatives displaying carboxylic acid functions in the pendant arms of the macrocycle were performed by oxidation of compound **9**. Despite different types of oxidant agents were used (KMnO_4 and $\text{K}_2\text{Cr}_2\text{O}_7$), the isolation of the desired product was not successfully achieved.

The synthesis of a cyclam derivative displaying cyanoethyl pendant arms was successfully achieved by reaction of **7** with an excess of acrylonitrile, as shown in Scheme 4.



Scheme 4. Reaction scheme of the synthesis of *trans*-di-di-substituted cyclam derivative **12**.

The ^1H NMR spectrum of **12** reveals a C_2 symmetric species with a pattern much like to the one observed for **11**.

Crystals of **12** suitable for single crystal X-ray diffraction were obtained by slow evaporation of a chloroform solution. Compound **12** crystallized in the monoclinic $\text{C}2/c$ space group with half molecule in the asymmetric unit. Crystallographic and experimental details of data collection and crystal structure determinations are presented in Table A4 (in Annex). The solid-state molecular structure of **12** reveals that the $^4\text{-CF}_3\text{PhCH}_2$ and $\text{CH}_2\text{CH}_2\text{CN}$ pendant arms are in mutually *trans* positions and are located at opposite sides of the macrocyclic ring (see Figure 12).

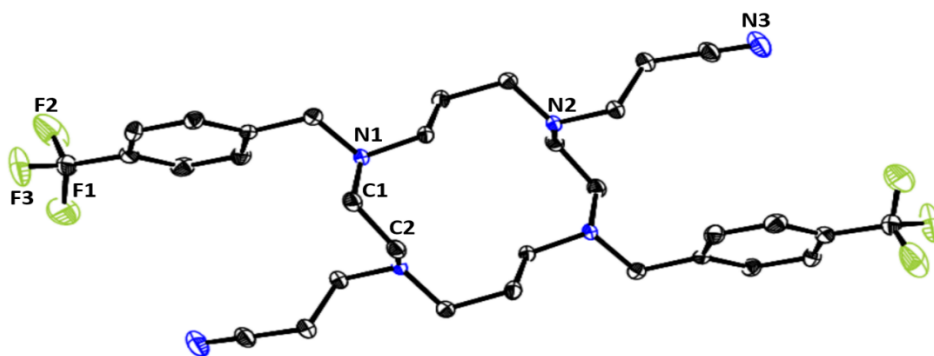


Figure 12. ORTEP diagram of $(\text{NCCH}_2\text{CH}_2)_2(^4\text{-CF}_3\text{PhCH}_2)_2\text{Cyclam}$, **12**, showing thermal ellipsoids at 40% probability level. Selected hydrogen atoms are omitted for clarity.

3.2. Incorporation of cyclam compounds in polymeric coatings

To verify the applicability of the synthesized cyclam compounds as antifouling agents in polymeric coatings for the protection of submerged surfaces against biofouling it is essential to incorporate them as additives (bioactive compounds) in the formulation of coatings or polymeric-based paints. This part of the work aimed to determine the concentration of compounds that matrices support and to select the compatible solvent for both matrix and compound to be incorporated. Thus, an iterative study of the different formulations of polymeric coatings for the matrix under study, polyurethane (PU), was carried out.

N-methyl-2-pyrrolidone was chosen as solvent because of its compatibility and common use in several painting formulations. However, previous studies revealed that, in the presence of cyclam-derived compounds, N-methyl-2-pyrrolidone promoted the loss of gloss of the obtained polymeric films and, in the specific case of the polyurethane-based matrix, it did not support concentrations higher than 1% (m/m) in wet formulations.^[14] Therefore, one of the main objectives of the present work is the development and optimization of the content of compound incorporated in polyurethane based matrices.

When it is mentioned that a compound or solvent is not compatible with the paint formulation, it means that apparent changes in at least one of main coating properties occurred when in comparison with its original formulation (without any additive added). Among these changes are loss of brightness, incomplete curing of the formed film, formation of agglomerates, loss of adhesion or colour change after the additive incorporation.

Table 5 shows the developed optimized polyurethane-based formulations containing the cyclam-derived compounds **7**, **9** and **11**.

Table 5. Optimized coating formulations containing cyclam-derived compounds **7**, **9** and **11**.

Polymeric matrix	Cyclam-derived compound	Solvent/compound ratio (m/m)	Base/curing agent ratio (m/m)	Content of cyclam-derived compound, % (m/m)
1 PU	2 REF	-	7.7 ± 1.3	-
	7	6.60 ± 1.14	7.8 ± 1.2	1.21 ± 0.03
	9	6.37 ± 0.90	8.0 ± 1.0	1.19 ± 0.05
	11	6.03 ± 0.56	8.0 ± 1.0	1.12 0.12

1. PU – Polyurethane; 2. REF – Control, the pristine PU coating without any cyclam derivative.

3.3. Evaluation of antimicrobial activity of coatings containing cyclam derived compounds

From the contact of both MRSA and *E. coli* bacteria with the reference PU coating and the biocidal coatings (coatings containing the compounds **7**, **9** and **11**), no significant antimicrobial effects were observed in all cases (Figure 13), since the normal growth for both MRSA and *E. coli* was not affected. In addition, no differences were seen between the reference free of bioactive

agents or the coatings with any of the cyclam-derivatives, **7**, **9** and **11**, as expressed by a yellowish opaque film. The compounds tested are expected to establish chemical bonds with isocyanate-based components of this polyurethane-based matrix through their $-NH$ and $-OH$ functions (section 3.4). The loss of bioactivity observed might suggest that those functions along with the presence of $-CF_3$ groups in the aromatic ring of the cyclam pending arms are both crucial to their antimicrobial properties.

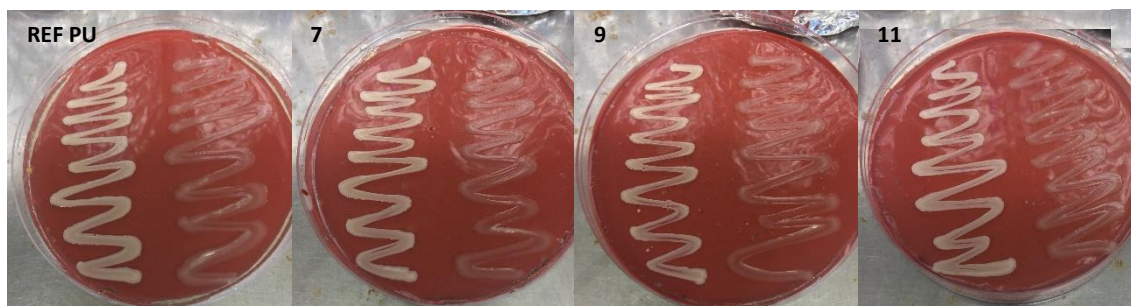


Figure 13. Antimicrobial assessment of coatings containing a reference (Ref PU) Petri dish and the optimized formulations of compounds **7**, **9** and **11** against MRSA (left side of petri dishes) and *E. coli* strains (right side of petri dishes).

3.4. Reaction of *trans*-di-substituted cyclam derivatives with MDI

The functionalization of cyclam derivatives **7** and **9** with isocyanate was attempted to evaluate the reactivity of the cyclam-derived compounds with the polymeric coating. Compounds were functionalized with 4,4'-methylenediphenyldiisocyanate (4,4'-MDI). The white precipitate formed was analysed by ATR-FTIR, mass spectrometry and elemental analysis.

The IR spectrum of the compound obtained from the reaction of **7** with 4,4'-MDI shown in Figure 14, reveals the presence of urea moieties due to the appearance of new bands: i) at 1636 cm^{-1} and 1593 cm^{-1} assigned to carbonyl ($-C=O$) stretching of amides; ii) at 1510 cm^{-1} assigned to the angular deformation of $-N-H$ which can be combined with the bending vibrations of $H-N-C=O$ Amide II (combined motion) and iii) at 1321 cm^{-1} and 1237 cm^{-1} assigned to the combination of $-C-C$ with $-C-N$ stretching.^{[55],[56]} The functionalization of the compound **7** also promoted the attenuation of the characteristic $-C-H$ stretching bands ranging from $2700-3000\text{ cm}^{-1}$.^[57]

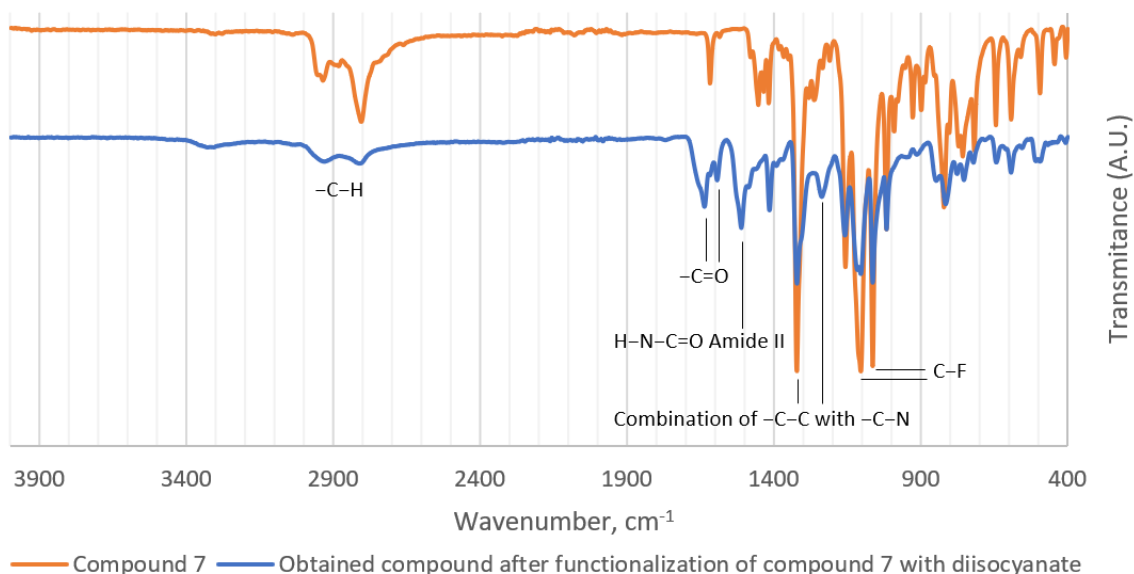


Figure 14. IR spectra of compound **7** (orange) and the obtained compound after functionalization of compound **7** with diisocyanate (blue).

The IR spectrum of the compound obtained from the reaction of **9** with 4,4'-MDI shown in Figure 15, clearly reveals the absence of the broad band ranging from 3075 to 3300 cm^{-1} , which was assigned to the -O-H stretching vibration (H-bonded) in **9**. On the other hand, the presence of the characteristic carbonyl (-C=O) stretching band around 1724 cm^{-1} , attributed to urethane bonds/secondary polyurethane structures, together with the characteristic -C-O stretching at 1220 cm^{-1} , and the -N-H deformation ranging from 1530-1510 cm^{-1} , suggests the presence of urethane moieties.

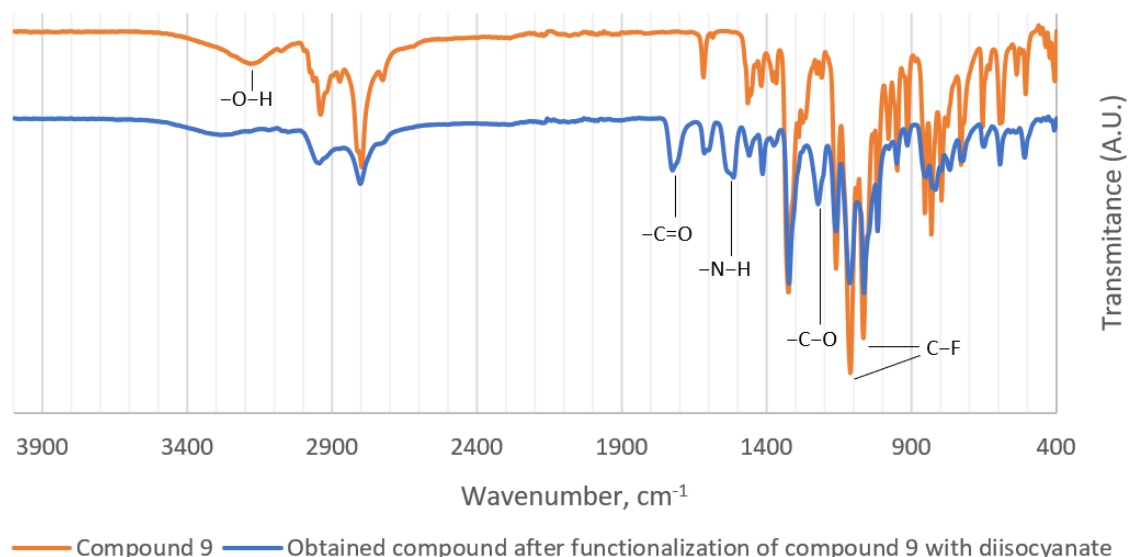


Figure 15. IR spectra of compound **9** (orange) and the obtained compound after functionalization of compound **9** with diisocyanate (blue).

The IR spectra of the products obtained from the reaction of the compounds **7** and **9** with the diisocyanate show intense absorption bands assigned to the C–F bonds stretching of CF₃ groups at 1105 cm⁻¹ and 1064 cm⁻¹ (for **7**, see Figure 14), and at 1111 cm⁻¹ and 1066 cm⁻¹ (for **9**, see Figure 15), confirming the presence of the cyclam backbone. The absence of the characteristic asymmetric stretch band of the isocyanate group (–N=C=O), in both products, in the range of 2276–2240 cm⁻¹ suggests that both isocyanate groups of 4,4'-MDI reacted with the cyclam-derived compounds under the tested reaction conditions.^{[58],[59]}

Despite the mass spectra of both products did not reveal molecular ions that correspond to a cyclam species linked to isocyanate fragments, the formation of such species cannot be ruled out.

Taking in consideration that both products display: i) poor solubility in the most common solvents; ii) the presence of new urea or urethane moieties; and iii) absence of free NCO fragments, it is plausible that reactions of the cyclam derivatives **7** and **9** with 4,4'-MDI might have led to the formation of the polymeric species like **13** and **14**, respectively, as shown in Figure 16.

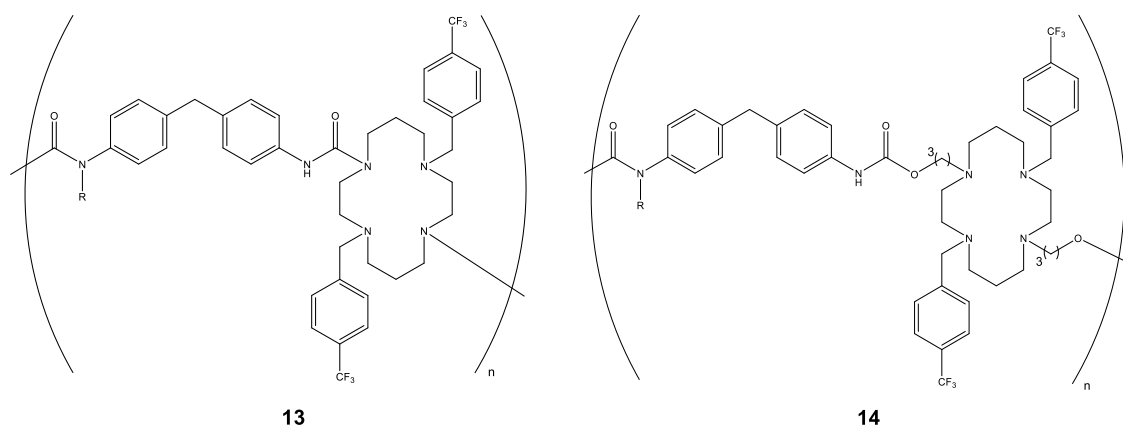


Figure 16. Proposed representative products obtained from the reaction of **7** and **9** with 4,4'-MDI.

3.5. Leaching tests

Leaching tests were performed on the optimized polyurethane-based formulations containing the cyclam-derived compounds incorporated.

After 45 days of submersion, the analysis of leaching waters obtained from formulations containing compounds **7**, **9** and **11** and control coated reference did not reveal the presence of cyclam-derived compounds. This result shows that the compounds are strongly immobilized to the coatings polymeric matrix.

This page was intentionally left blank.

4. Conclusions

The antimicrobial assessment in this polyurethane-based matrix against both MRSA and *E. coli* disclose that the normal bacteria growth was not affected since no differences were seen between the reference or the coatings with any of the compounds, **7**, **9** and **11**.

It was observed that the incorporation of cyclam-derived compounds in polyurethane is strongly bonded being not detected in leaching water after 45 days of immersion. The reaction with the 4,4'-MDI revealed the formation of urethane and urea-type bonds that strongly bind the compounds to the paint polymeric matrix.

In conclusion, cyclam-derived compounds are potential antimicrobial agents to be applied as bioactive additives in silicone-based paints.^[14] However, for high chemical compatibility of cyclam-derivatives with polymeric matrices, such as polyurethane-based coatings, a loss of antimicrobial activity is observed due the strong chemical binding of the compounds with the matrices through the -NH and -OH groups. This structure/activity relationship reveals that the presence of -NH and -OH functions along with the presence of -CF₃ groups in the aromatic ring of the cyclam pending arms are both crucial to their antimicrobial properties.

This page was intentionally left blank.

References

- [1] O. Griffiths, H. Henderson, and M. Simpson, *Environmental Health Practitioner Manual*. 2010.
- [2] L. Baroni, L. Cenci, M. Tettamanti, and M. Berati, "Evaluating the environmental impact of various dietary patterns combined with different food production systems," *Eur. J. Clin. Nutr.*, vol. 61, no. 2, pp. 279–286, 2007, doi: 10.1038/sj.ejcn.1602522.
- [3] H. Ritchie and M. Roser, "Water Use and Stress," *Our World Data*, Nov. 2017, Accessed: Nov. 16, 2020. [Online]. Available: <https://ourworldindata.org/water-use-stress>.
- [4] "Water Pollution Facts, Types, Causes and Effects of Water Pollution | NRDC." <https://www.nrdc.org/stories/water-pollution-everything-you-need-know#whatis> (accessed Sep. 19, 2020).
- [5] E. Koncagül, M. Tran, R. Connor, S. Uhlenbrook, and A. Renata Cordeiro Ortigara, "Wastewater: The Untapped Resource," 2017.
- [6] WWAP, "The United Nations world water development report 2018: nature-based solutions for water; 2018," 2018. Accessed: Nov. 16, 2020. [Online]. Available: <https://unesdoc.unesco.org/ark:/48223/pf0000261424/PDF/261424eng.pdf.multi>.
- [7] "WHO | Diseases and risks." https://www.who.int/water_sanitation_health/diseases-risks/en/ (accessed Sep. 02, 2020).
- [8] E. Ezalia *et al.*, "World Health Statistics 2020: Monitoring Health For the SDGs," 2020. doi: 10.1155/2010/706872.
- [9] "884 milhões de pessoas ainda sem acesso a água potável – Observador." <https://observador.pt/2017/07/12/884-milhoes-de-pessoas-ainda-sem-acesso-a-agua-potavel/> (accessed Oct. 14, 2020).
- [10] D. Pooja, P. Kumar, P. Singh, and S. Patil, *Sensors in Water Pollutants Monitoring: Role of Material*. Springer Nature Singapore Pte Ltd. 2020, 2020.
- [11] WHO, "Microbial Aspects," *WHO Guidel. Drink. Qual.*, vol. 38, no. Chapter 2, pp. 117–153, 2011, [Online]. Available: <http://www.ncbi.nlm.nih.gov/pubmed/15806952>.
- [12] J. C. Crittenden, R. R. Trussell, D. W. Hand, K. J. Howe, and G. Tchobanoglous, *MWH's Water Treatment Principles and Design*, Third Edit. 2012.
- [13] US Environmental Protection Agency, "The History of Drinking Water Treatment," *Public Health*, vol. 40, no. 4606, pp. 1–4, 2000, [Online]. Available: <http://www.epa.gov/ogwdw000/consumer/pdf/hist.pdf>.
- [14] S. Almada, "Compostos derivados de ciclama para a bio-descontaminação da água", Thesis, Instituto Superior Técnico, 2019.
- [15] "Aeration | How does it work | Advantages and Disadvantages." <https://www.zuiveringstechnieken.nl/Aeration> (accessed Nov. 18, 2020).
- [16] "Activated carbon adsorption | EMIS." <https://emis.vito.be/nl/node/19448> (accessed Nov. 18, 2020).
- [17] C. M. Magin, S. P. Cooper, and A. B. Brennan, "Non-toxic antifouling strategies," *Mater. Today*, vol. 13, no. 4, pp. 36–44, 2010, doi: 10.1016/S1369-7021(10)70058-4.

- [18] K. A. Dafforn, J. A. Lewis, and E. L. Johnston, "Antifouling strategies: History and regulation, ecological impacts and mitigation," *Mar. Pollut. Bull.*, vol. 62, no. 3, pp. 453–465, 2011, doi: 10.1016/j.marpolbul.2011.01.012.
- [19] J. A. Callow and M. E. Callow, "Trends in the development of environmentally friendly fouling-resistant marine coatings," *Nat. Commun.*, vol. 2, no. 1, pp. 210–244, 2011, doi: 10.1038/ncomms1251.
- [20] A. J. Martín-Rodríguez *et al.*, "From broad-spectrum biocides to quorum sensing disruptors and mussel repellents: Antifouling profile of alkyl triphenylphosphonium salts," *PLoS One*, vol. 10, no. 4, 2015, doi: 10.1371/journal.pone.0123652.
- [21] O. Ferreira *et al.*, "Biofouling Inhibition with Grafted Econea Biocide: Toward a Nonreleasing Eco-Friendly Multiresistant Antifouling Coating," *ACS Sustain. Chem. Eng.*, vol. 8, no. 1, pp. 12–17, 2020, doi: 10.1021/acssuschemeng.9b04550.
- [22] S. B. Choi, J. Jepperson, L. Jarabek, J. Thomas, B. Chisholm, and P. Boudjouk, "Novel approach to anti-fouling and fouling-release marine coatings based on dual-functional siloxanes," *Macromol. Symp.*, vol. 249–250, pp. 660–667, 2007, doi: 10.1002/masy.200750452.
- [23] J. P. Maréchal and C. Hellio, "Challenges for the development of new non-toxic antifouling solutions," *Int. J. Mol. Sci.*, vol. 10, no. 11, pp. 4623–4637, 2009, doi: 10.3390/ijms10114623.
- [24] D. M. Yebra, S. Kiil, and K. Dam-Johansen, "Antifouling technology - Past, present and future steps towards efficient and environmentally friendly antifouling coatings," *Prog. Org. Coatings*, vol. 50, no. 2, pp. 75–104, 2004, doi: 10.1016/j.porgcoat.2003.06.001.
- [25] "Marine Growth Prevention System (MGPS) - Anti Fouling System." <https://cathodicme.com/mgps-systems/marine-growth-prevention-system/> (accessed Nov. 17, 2020).
- [26] N. R. Council, *Drinking Water and Health: Volume 4. IV Biological Quality of Water in the Distribution System*. Washington, DC: The National Academies Press, 1982.
- [27] D. of Agriculture, "Anti-fouling and in-water cleaning guidelines," 2015. [Online]. Available: agriculture.gov.au.
- [28] M. Cloutier, D. Mantovani, and F. Rosei, "Antibacterial Coatings: Challenges, Perspectives, and Opportunities," *Trends Biotechnol.*, vol. 33, no. 11, pp. 637–652, 2015, doi: 10.1016/j.tibtech.2015.09.002.
- [29] E. R. Silva *et al.*, "Eco-friendly non-biocide-release coatings for marine biofouling prevention," *Sci. Total Environ.*, vol. 650, pp. 2499–2511, 2019, doi: 10.1016/j.scitotenv.2018.10.010.
- [30] Y. H. Pang, "Antimicrobial and Anti-adhesion Coating on Water Filtration Membrane," Hong Kong University of Science and Technology, 2015.
- [31] E. R. Silva, O. Ferreira, P. Rijo, J. C. Bordado, and M. J. Calhorda, "Antifouling Eco-Filters for Water Bio-Econtamination," *Proceedings*, vol. 2, no. 5, p. 181, 2017, doi: 10.3390/ecws-2-04950.
- [32] "The Colorful History of Paint | EarthDate." <https://www.earthdate.org/colorful-history-of-paint> (accessed Oct. 27, 2020).
- [33] F. Marques, "Tecnologias de aplicação de pinturas e patologias em paredes de alvenaria e elementos de betão", Thesis, Instituto Superior Técnico, 2013.

- [34] A. Spurgeon, "Watching paint dry: Organic solvent syndrome in late-twentieth-century Britain," *Med. Hist.*, vol. 50, no. 2, pp. 167–188, 2006, doi: 10.1017/S002572730000973X.
- [35] R. Feio, "Microcápsulas com função biocida para o controlo da bioincrustação", Thesis, Instituto Superior Técnico, 2015.
- [36] "ISO - ISO 4618:2014 - Paints and varnishes — Terms and definitions." <https://www.iso.org/standard/56502.html> (accessed Nov. 20, 2020).
- [37] "Classification of paints." http://www.substech.com/dokuwiki/doku.php?id=classification_of_paints (accessed Oct. 27, 2020).
- [38] Michigan State University (institution), "Major Action Modes of Antimicrobial Drugs," *Pharmacol. Modul.*, pp. 6–16, 2011, [Online]. Available: <http://amrls.cvm.msu.edu/pharmacology/antimicrobials/antimicrobials-an-introduction>.
- [39] A. Prokhorov, H. Bernard, N. Le Bris, N. Marquet, and H. Handel, "Synthesis of a new ditopic ligand possessing linear and cyclic tetraaza subunits," *Synth. Commun.*, vol. 38, no. 10, pp. 1589–1600, 2008, doi: 10.1080/00397910801929481.
- [40] T. Fe, "Electronic Supplementary Information," *Scanning*, no. 25 mL, pp. 1–10, 2011.
- [41] O. Semana, "Octava Semana.1," *European J. Org. Chem.*, vol. 1, no. 2000, p. 200004, 2005, [Online]. Available: [http://doi.wiley.com/10.1002/\(SICI\)1099-0690\(199809\)1998:9%3C1971::AID-EJOC1971%3E3.0.CO;2-D%5Cn%3CGo to ISI%3E://000075809400031](http://doi.wiley.com/10.1002/(SICI)1099-0690(199809)1998:9%3C1971::AID-EJOC1971%3E3.0.CO;2-D%5Cn%3CGo to ISI%3E://000075809400031).
- [42] L. G. Alves, M. T. Duarte, and A. M. Martins, "Structural features of neutral and cationic cyclams," *J. Mol. Struct.*, vol. 1098, pp. 277–288, 2015, doi: 10.1016/j.molstruc.2015.05.037.
- [43] L. G. Alves, P. F. Pinheiro, J. R. Feliciano, D. P. Dâmaso, J. H. Leitão, and A. M. Martins, "Synthesis, antimicrobial activity and toxicity to nematodes of cyclam derivatives," *Int. J. Antimicrob. Agents*, vol. 49, no. 5, pp. 646–649, 2017, doi: 10.1016/j.ijantimicag.2017.03.002.
- [44] A. Pilon *et al.*, "New Cyclams and Their Copper(II) and Iron(III) Complexes: Synthesis and Potential Application as Anticancer Agents," *ChemMedChem*, vol. 14, no. 7, pp. 770–778, 2019, doi: 10.1002/cmdc.201800702.
- [45] Bruker, "SAINT+." Bruker AXS Inc., Madison, Wisconsin, USA, 2007.
- [46] G. M. Sheldrick, "SADABS." University of Göttingen, Germany, 1996.
- [47] A. Altomare *et al.*, "SIR97: A new tool for crystal structure determination and refinement," *J. Appl. Crystallogr.*, vol. 32, no. 1, pp. 115–119, 1999, doi: 10.1107/S0021889898007717.
- [48] M. C. Burla *et al.*, "SIR2004: An improved tool for crystal structure determination and refinement," *J. Appl. Crystallogr.*, vol. 38, no. 2, pp. 381–388, 2005, doi: 10.1107/S002188980403225X.
- [49] G. M. Sheldrick, "A short history of SHELX," *Acta Crystallogr. Sect. A Found. Crystallogr.*, vol. 64, no. 1, pp. 112–122, 2008, doi: 10.1107/S0108767307043930.
- [50] L. J. Farrugia, "WinGX and ORTEP for Windows: An update," *J. Appl. Crystallogr.*, vol. 45, no. 4, pp. 849–854, 2012, doi: 10.1107/S0021889812029111.
- [51] C. F. Macrae *et al.*, "Mercury CSD 2.0 - New features for the visualization and investigation of crystal structures," *J. Appl. Crystallogr.*, vol. 41, no. 2, pp. 466–470, 2008, doi: 10.1107/S0021889807067908.

- [52] L. G. Alves *et al.*, "Investigations into the structure/antibacterial activity relationships of cyclam and cyclen derivatives," *Antibiotics*, vol. 8, no. 4, 2019, doi: 10.3390/antibiotics8040224.
- [53] U. Schoknecht, J. Gruycheva, H. Mathies, H. Bergmann, and M. Burkhardt, "Leaching of biocides used in façade coatings under laboratory test conditions," *Environ. Sci. Technol.*, vol. 43, no. 24, pp. 9321–9328, 2009, doi: 10.1021/es9019832.
- [54] F. H. Allen, O. Kennard, D. G. Watson, L. Brammer, A. G. Orpen, and R. Taylor, "Tables of bond lengths determined by x-ray and neutron diffraction. Part 1. Bond lengths in organic compounds," *J. Chem. Soc. Perkin Trans. 2*, no. 12, pp. 1–19, 1987, doi: 10.1039/P29870000051.
- [55] S. Radice and M. Bradley, "Time-Based FT-IR Analysis of Curing of Polyurethanes," *Thermo Sci. Appl. Note*, no. 51255, pp. 1–3, 2013, [Online]. Available: <http://www.thermoscientific.com/ecommservlet/techresource?storeId=11152&langId=-1&taxonomy=4&resourceId=81104&contentType=Application+Notes&productId=11961710#>.
- [56] F. Mallamace, C. Corsaro, D. Mallamace, S. Vasi, C. Vasi, and G. Dugo, "The role of water in protein's behavior: The two dynamical crossovers studied by NMR and FTIR techniques," *Comput. Struct. Biotechnol. J.*, vol. 13, pp. 33–37, 2015, doi: 10.1016/j.csbj.2014.11.007.
- [57] I. L. Vera-Estrada, J. Uribe-Godínez, and O. Jiménez-Sandoval, "Study of M(iii)-cyclam (M = Rh, Ru; Cyclam = 1,4,8,11-tetraazacyclotetradecane) complexes as novel methanol resistant electrocatalysts for the oxygen reduction reaction," *RSC Adv.*, vol. 10, no. 38, pp. 22586–22594, 2020, doi: 10.1039/d0ra02904a.
- [58] R. M. Silverstien, F. X. Webster, and D. J. Kiemle, *Spectrometric Identification of Organic Compounds*, Seventh Ed. New York: John Wiley & Sons, Inc., 2005.
- [59] J. Coates, "Interpretation of Infrared Spectra, A Practical Approach," *Encycl. Anal. Chem.*, pp. 1–23, 2006, doi: 10.1002/9780470027318.a5606.

Annexes

Table A1. Crystal data and structure refinement for **8**.

Empirical formula	C34 H46 F6 N4 O4	
Formula weight	688.75	
Temperature (K)	150(2)	
Wavelength (Å)	0.71073	
Crystal system, space group	Triclinic, P-1	
Unit cell dimensions	a (Å) = 9.258(2)	α (°) = 86.34(1)
	b (Å) = 9.906(2)	β (°) = 74.155(9)
	c (Å) = 10.738(2)	γ (°) = 64.368(8)
Volume (Å ³)	852.5(3)	
Z	1	
Calculated density (g.cm ⁻³)	1.342	
Absorption coefficient (mm ⁻¹)	0.110	
<i>F</i> (000)	364	
Crystal size (mm)	0.06 x 0.10 x 0.30	
θ range for data collection (°)	2.577 to 25.680	
Limiting indices	-11 ≤ <i>h</i> ≤ 11, -11 ≤ <i>k</i> ≤ 12, -12 ≤ <i>l</i> ≤ 13	
Reflections collected/unique	8099 / 3181 [<i>R</i> _{int} = 0.0646]	
Completeness to θ (%)	98.2	
Absorption correction	Multi-scan	
Refinement method	Full-matrix least-squares on <i>F</i> ²	
Data / restraints / parameters	3181 / 0 / 218	
Goodness-of-fit on <i>F</i> ²	1.011	
Final <i>R</i> indices [<i>I</i> > 2 σ (<i>I</i>)]	<i>R</i> ₁ = 0.0753, ωR ₂ = 0.1843	
<i>R</i> indices (all data)	<i>R</i> ₁ = 0.1438, ωR ₂ = 0.2063	
Largest diff. peak and hole (eÅ ⁻³)	0.392 and -0.338	

$$R_1 = \frac{\sum ||F_0| - |F_c||}{\sum |F_0|}$$

$$\omega R_2 = \left[\frac{\sum \omega (F_0^2 - F_c^2)^2}{\sum \omega (F_0^2)^2} \right]^{\frac{1}{2}}$$

Table A2. Crystal data and structure refinement for **10**.

Empirical formula	C34 H46 F6 N4 O4	
Formula weight	688.75	
Temperature (K)	150(2)	
Wavelength (Å)	0.71073	
Crystal system, space group	Triclinic, P-1	
Unit cell dimensions	a (Å) = 5.3622(7)	α (°) = 95.539(8)
	b (Å) = 8.688(1)	β (°) = 91.382(8)
	c (Å) = 19.054(2)	γ (°) = 105.270(7)
Volume (Å ³)	851.19(18)	
Z	1	
Calculated density (g.cm ⁻³)	1.344	
Absorption coefficient (mm ⁻¹)	0.110	
<i>F</i> (000)	364	
Crystal size (mm)	0.06 x 0.16 x 0.20	
θ range for data collection (°)	1.075 to 25.755	
Limiting indices	-6 ≤ <i>h</i> ≤ 6, -10 ≤ <i>k</i> ≤ 10, -22 ≤ <i>l</i> ≤ 22	
Reflections collected/unique	5551 / 3028 [<i>R</i> _{int} = 0.0456]	
Completeness to θ (%)	93.2	
Absorption correction	Multi-scan	
Refinement method	Full-matrix least-squares on <i>F</i> ²	
Data / restraints / parameters	3028 / 0 / 218	
Goodness-of-fit on <i>F</i> ²	1.053	
Final <i>R</i> indices [<i>I</i> > 2 σ (<i>I</i>)]	<i>R</i> ₁ = 0.0993, ωR ₂ = 0.2686	
<i>R</i> indices (all data)	<i>R</i> ₁ = 0.1745, ωR ₂ = 0.3110	
Largest diff. peak and hole (eÅ ⁻³)	0.597 and -0.671	

$$R_1 = \frac{\sum ||F_0| - |F_c||}{\sum |F_0|}$$

$$\omega R_2 = \left[\frac{\sum \omega (F_0^2 - F_c^2)^2}{\sum \omega (F_0^2)^2} \right]^{\frac{1}{2}}$$

Table A3. Crystal data and structure refinement for **11**.

Empirical formula	C30 H42 F6 N4 O2	
Formula weight	604.68	
Temperature (K)	150(2)	
Wavelength (Å)	0.71073	
Crystal system, space group	Triclinic, P-1	
Unit cell dimensions	a (Å) = 8.930(1)	α (°) = 91.972(5)
	b (Å) = 9.2703(9)	β (°) = 106.372 (6)
	c (Å) = 9.6657(9)	γ (°) = 101.663(5)
Volume (Å ³)	748.30(13)	
Z	1	
Calculated density (g.cm ⁻³)	1.342	
Absorption coefficient (mm ⁻¹)	0.110	
<i>F</i> (000)	320	
Crystal size (mm)	0.08 x 0.12 x 0.14	
θ range for data collection (°)	2.207 to 26.467	
Limiting indices	-11 ≤ <i>h</i> ≤ 11, -10 ≤ <i>k</i> ≤ 11, -12 ≤ <i>l</i> ≤ 10	
Reflections collected/unique	6863 / 3078 [<i>R</i> _{int} = 0.0455]	
Completeness to θ (%)	99.8	
Absorption correction	Multi-scan	
Refinement method	Full-matrix least-squares on <i>F</i> ²	
Data / restraints / parameters	3078 / 0 / 194	
Goodness-of-fit on <i>F</i> ²	1.077	
Final <i>R</i> indices [<i>I</i> > 2 σ (<i>I</i>)]	<i>R</i> ₁ = 0.0633, ωR ₂ = 0.1540	
<i>R</i> indices (all data)	<i>R</i> ₁ = 0.0969, ωR ₂ = 0.1671	
Largest diff. peak and hole (eÅ ⁻³)	0.616 and -0.528	

$$R_1 = \frac{\sum ||F_0| - |F_c||}{\sum |F_0|}$$

$$\omega R_2 = \left[\frac{\sum \omega (F_0^2 - F_c^2)^2}{\sum \omega (F_0^2)^2} \right]^{\frac{1}{2}}$$

Table A4. Crystal data and structure refinement for **12**.

Empirical formula	C32 H40 F6 N6	
Formula weight	622.70	
Temperature (K)	150(2)	
Wavelength (Å)	0.71073	
Crystal system, space group	Monoclinic, C2/c	
Unit cell dimensions	a (Å) = 25.328(2)	α (°) = 90
	b (Å) = 5.7081(5)	β (°) = 118.384(4)
	c (Å) = 24.491(2)	γ (°) = 90
Volume (Å ³)	3115.1(5)	
Z	4	
Calculated density (g.cm ⁻³)	1.328	
Absorption coefficient (mm ⁻¹)	0.105	
<i>F</i> (000)	1312	
Crystal size (mm)	0.06 x 0.10 x 0.18	
θ range for data collection (°)	1.905 to 27.180	
Limiting indices	-32 ≤ <i>h</i> ≤ 32, -7 ≤ <i>k</i> ≤ 7, -26 ≤ <i>l</i> ≤ 31	
Reflections collected/unique	10078 / 3457 [<i>R</i> _{int} = 0.0579]	
Completeness to θ (%)	99.9	
Absorption correction	Multi-scan	
Refinement method	Full-matrix least-squares on <i>F</i> ²	
Data / restraints / parameters	3457 / 0 / 199	
Goodness-of-fit on <i>F</i> ²	1.050	
Final <i>R</i> indices [<i>I</i> > 2 σ (<i>I</i>)]	<i>R</i> ₁ = 0.0642, ωR ₂ = 0.1533	
<i>R</i> indices (all data)	<i>R</i> ₁ = 0.1257, ωR ₂ = 0.1729	
Largest diff. peak and hole (eÅ ⁻³)	0.674 and -0.397	

$$R_1 = \frac{\sum \|F_0\| - \|F_c\|}{\sum \|F_0\|} \quad \omega R_2 = \left[\frac{\sum \omega (F_0^2 - F_c^2)^2}{\sum \omega (F_0^2)^2} \right]^{\frac{1}{2}}$$